Electronic Supplementary Material (ESI) for Nanoscale.

Photosensitizer Localization in Amphiphilic Block Copolymers Controls Photodynamic Therapy Efficacy

Vusala Ibrahimova, Sergey A. Denisov, Kevin Vanvarenberg, Peter Verwilst, Véronique Préat, Jean-Michel Guigner, Nathan D. McClenaghan, Sébastien Lecommandoux and Charles-Andre Fustin**

Table of Contents

1. Experimental Procedures

1.1 Materials

The following reagents were used without further purification: diethyl amine ($(C_2H_5)_2NH$, Sigma-Aldrich, 99.5%), 1,3-diiodopropane ($I(CH_2)_3I$, Sigma-Aldrich, purum 97.0%), potassium tert-butoxide (KOtBu, Fluka, purum 99%), tert-Butyl bromoacetate ($BrCH_2COOC(CH_3)_3$, Sigma-Aldrich, 98%), N,N-diisopropylethylamine (DIPEA, Sigma-Aldrich, 99%), boron trifluoride etherate ($BF_3{\cdot}OEt_2$, TCI, 98%), trifluoroacetic acid ($C_2HF_3O_2$, TCI, 99%), N-bromosuccinimide (NBS, Sigma-Aldrich, 99%), sodium bicarbonate ($NaHCO_3$, ACS reagent, 99.7+%), 1-hydroxybenzotriazole hydrate (HOBt, Sigma-Aldrich, 97%), 1-(3-dimethylaminopropyl)-3-ethylcarbodiimide hydrochloride (EDCI, Acros Organics, 98+%), poly(ethylene oxide) methyl ether (Mn = 2000, 5000 g/mol, Aldrich), sodium sulfate (Na_2SO_4, VWR, 98%), potassium carbonate (K_2SO_4, VWR), magnesium sulfate ($MgSO_4$, VWR), tris(benzyltriazolylmethyl)amine (TBTA, TCI, 97%), ethylenediaminetetraacetic acid disodium salt dihydrate (EDTA, ACS reagent, 99%), triethylamine (TEA, Merck Schuchardt OHG, pharma grade), glacial acetic acid (CH_3CO_2H, Chem-Labs Limited), hydrochloric acid (HCl, VWR, 37%), tetrabutylammonium fluoride (TBAF, 1 M solution in THF, TCI chemicals), azidotrimethylsilane ($TMSN_3$, Alfa Aesar, 94%), copper(I) sulfate (Cu_2SO_4, Acros Organics, 98%), copper(I) bromide (CuBr, Acros Organics, 98%), L-Ascorbic acid sodium salt ($C_6H_7NaO_6$, Acros Organics, 99%), bio-beads TM S-X1 (BIO-RAD, 200-400 mesh), silica gel 60A (SiO_2, 230-400 mesh ASTM, ROCC, 99.5%), ϒ-benzyl-L-glutamate N-carboxyl anhydride (NCA-BLG, Isochem France), ruthenium (III) chloride ($RuCl_3.x\ H_2O$, Sigma-Aldrich, >99.8%), iodine (I_2, Sigma-Aldrich, >99.8%), 3,7-bis(dimethylamino)-5-phenothiazinium chloride hydrate (Methylene blue, Sigma-Aldrich, 82%), minimum essential medium (MEM, Thermo Fisher Scientific), minimum essential medium (MEM Alpha Medium (1X) + GlutaMax, Thermo Fisher Scientific), 3-[4,5-dimethylthiazol-2-yl]-2,5- diphenyltetrazolium bromide (thiazolyl blue; MTT, Sigma-Aldrich), phosphate-buffered saline (PBS, Thermo Fisher Scientific), 4′,6-diamidino-2-phenylindole (DAPI, Thermo Fisher Scientific). Chain end functionalized PEGs were obtained from literature procedures,[1a,b] as were the singlet oxygen trap, 9,10-bis- (vinylsulfonate)anthracene (AVS)[2b] and benchmark Aza-BODIPY **5.**[2a]

The following solvents have been used without further purification: ethanol (EtOH, VWR chemicals, analytical grade, 100%), dichloromethane (DCM, Sigma-Aldrich, analytical grade, 99.9%), n-hexane (C_6H_{14}, Sigma-Aldrich, analytical grade, 97%), extra pure 99+%), N,N-dimethylformamide (DMF, Fluka, 99.8%), acetonitrile (ACN, VWR chemicals, HPLC grade, 99.9%), tetrahydrofuran (THF, Fluka, 99.8%), ethyl acetate (EtOAc, Sigma-Aldrich, 99.5%), acetone ($(CH_3)_2CO$, Sigma-Aldrich, 99.5%), diethyl ether (Et_2O, VWR chemicals, 97%), dimethyl sulfoxide (DMSO, Sigma-Aldrich, 99,9%). In photophysical characterizations, tetrahydrofuran (THF, Fluka, 99.8%) was used after distillation over CaH_2.

1.2 Methods

Nuclear Magnetic Resonance (NMR): ^1H, ^{13}C and ^{11}B NMR 500 MHz spectra have been taken with a Bruker 500 MHz Avance. ^1H NMR 300 MHz spectra have been taken with a Bruker 300 MHz Avance II. ^1H NMR 400 MHz spectra have been taken with a Bruker Avance DPX 400. Deuterated chloroform ($CDCl_3$, Euriso-top, 99.8%) and deuterated acetone ($(CD_3)_2O$, Euriso-top, 99.8%),) have been used as solvent and reference for the lock.

Size Exclusion Chromatography (SEC): Analyses by SEC were performed on an Agilent gel permeation chromatography system and on Varian system. Agilent SEC was equipped with RI and UV detectors, an Agilent 1100/1200 pump (35°C; eluent: DMF 2.5 mM of NH_4PF_6; flow rate of 1 mL/min), and two PSS GRAM columns (beads 10 µm; porosity of column 1, 1000 Å; porosity of column 2, 100 Å). The calibration was performed using PEO standards.

Analytical thin-layer chromatography (TLC) was performed on alumina plates coated with silica gel GF254 (Merck, 0.22 mm thick)

Mass Spectrometry (MS): high resolution mass spectrometry analyses were performed on a ThermoScientific Q-Exactive mass spectrometer in ESI (electrospray ionization) or APCI (atmospheric-pressure chemical ionization) mode.

A**ttenuated total reflection Fourier transform infrared spectroscopy** (ATR FTIR): FTIR spectra were recorded directly on a powder samples at 400-4000 cm^{-1} (resolution of 4 cm^{-1}) range by using attenuated total reflection mode.

Fluorescence spectroscopy: fluorescence and phosphorescence emission spectra of optically diluted solutions were recorded on a Horiba Jobin-Yvon Fluorolog-3 spectrofluorometer with TCSPC capability. It is equipped with photomultipliers from Hamamatsu Photonics R2658 (280-1100 nm range) and R928 (280-950 nm range), iHR-320 spectrograph (150-1500 nm range, 1200 gr/mm grating, blazed at 500 nm) and NIR detector H10330-45 (950-1400 nm range). For routine fluorescence measurements a Fluorimeter Varian Cary Eclipse was used.

LED Array: High Power 660 nm Red 32 LED Array (power density 1.33 mW/cm^2) was purchased from ELIXA (http://www.elixa.com/).

Transient absorption/ time-resolved fluorescence: Sub-nanosecond set-up (Figure S1) was built at the Institut des Sciences Moléculaires (ISM), University of Bordeaux as follows. A frequency tripled Nd:YAG amplified laser system (30 ps, 30 mJ @1064 nm, 20 Hz, Ekspla model PL 2143) output was used to pump an optical parametric generator (Ekspla model PG 401) producing tunable excitation pulses in the range 410-2300 nm. The white light pulse for sample probing was produced by focusing the residual fundamental laser radiation to high pressure Xe filled breakdown cell. All light signals were analyzed by a spectrograph (Princeton Instruments Acton model SP2300) coupled with a high dynamic range streak camera (Hamamatsu C7700). Accumulated sequences (sample emission, probe without and with excitation) of pulses were recorded and treated by HPDTA (Hamamatsu) software to

produce two-dimensional maps (wavelength *vs* delay) of transient absorption intensity in the range 300-800 nm. The typical measurement error is 10^{-3} OD.[2a,3] The schematic illustration of the set-up is shown below.

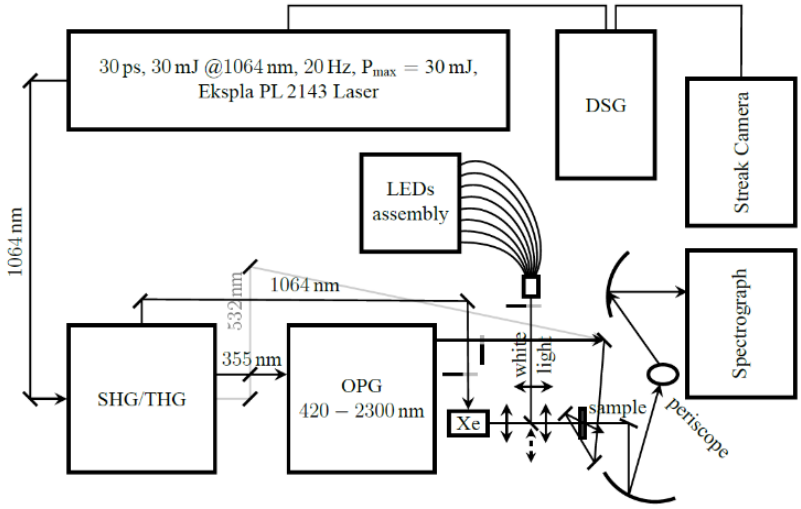

Figure S1. Sub-nanosecond laser set-up; DSG digital signal generator, SHG/THG second/third harmonic generator, LED light emitting diode and OPG optical parametric generator[3]

Dynamic light scattering: Hydrodynamic radius (R_h) of the nanocarriers was measured by dynamic light scattering (DLS) which was carried out with a Malvern CGS3 device equipped with a He-Ne laser at a wavelength of 632.8 nm. Measurements were performed at 25°C at an angle of 90° with an acquisition time of 30 s. Results were analyzed using the CONTIN algorithm to obtain size distribution and with the cumulant method to obtain the polydispersity index (PDI).

Cryo Transmission Electron Microscopy: A drop (5 µL) of the suspension was deposited on a Lacey carbon grid. The excess of solution was then blotted out with a filter paper, and before evaporation the grid was quench-frozen in liquid ethane to form a thin vitreous ice film. The grid was then mounted in a Gatan 626 cryo-holder (Gatan, USA) cooled with liquid nitrogen and transferred in the Cryo microscope. Cryo-TEM images were taken on an Ultrascan 2k CCD camera (Gatan, USA), using a LaB_6 JEOL JEM 2100 (JEOL, Japan) cryo-microscope operating at 200kV with a JEOL low dose system (Minimum Dose System, MDS) to protect the thin ice film from any irradiation before imaging and reduce the irradiation during the image capture. The images were taken at 96 K.

Fluorescence microscopy: The HeLa and B16F1 cells were seeded in a cover slip containing 12-well plates (10^5 cells/well) and incubated for 24 h. The cells were then incubated with the nanocarriers for 24 h with 1 mg/mL concentration, then fixed with fresh paraformaldehyde (2% (w/v) in PBS) and rinsed three times with PBS solution. The cell nuclei was stained by 4′,6-diamidino-2-phenylindole (DAPI; 0.1 µg/mL). After 5 min incubation, the cells were rinsed with PBS solution three times. The cells were incubated for 1 h with AlexaFluor488-conjugated concanavalin A (5 µg/mL in PBS, Molecular Probes) to stain the cell membranes. After washing, the cover slips were placed on a slide using the Vectashield® mounting medium. The slides were imaged using a structured illumination AxioImager microscope equipped with an Apotome module (Zeiss, Germany, magnification 40×).

Titration: The primary amine yields in the polypeptide chain-end were calculated with basic acid-base titration method. 100 mg of polymer samples were dissolved in DCM/Acetic acid mixture (1 mL DCM/ 2 mL Acetic acid), a few drops of crystal violet were added and followed by acid titration (0.005 M perchloric acid in acetic acid 100%).

General procedure of self-assembly: All self-assembled nanoparticle solutions were prepared at 4mg/mL concentration in Milli-Q water. Amphiphilic block copolymers bearing photosensitizer, PS-$PBLG_{49}$-*b*-PEG_{45} and $PBLG_{53}$-PS-*b*-PEG_{45}, were co-assembled with PS free amphiphilic block copolymers $PBLG_{54}$-*b*-PEG_{45} in 1:1 weight ratio. 4 mg of PS functionalized and non-functionalized polymer mixtures (1:1 w/w) were dissolved in 200 µL THF and stirred for 30 min. 1 mL of Milli-Q water was added at a flow rate of 0.37 mL/min with a syringe pump and with a stirring speed of 500 rpm. The solution was stirred for 5 min, transferred to a dialysis bag (cut-off MWCO 12-14 kDa) and dialyzed for 24 h, changing the water every 6 h.

2. Results and Discussion

2.1 Synthesis

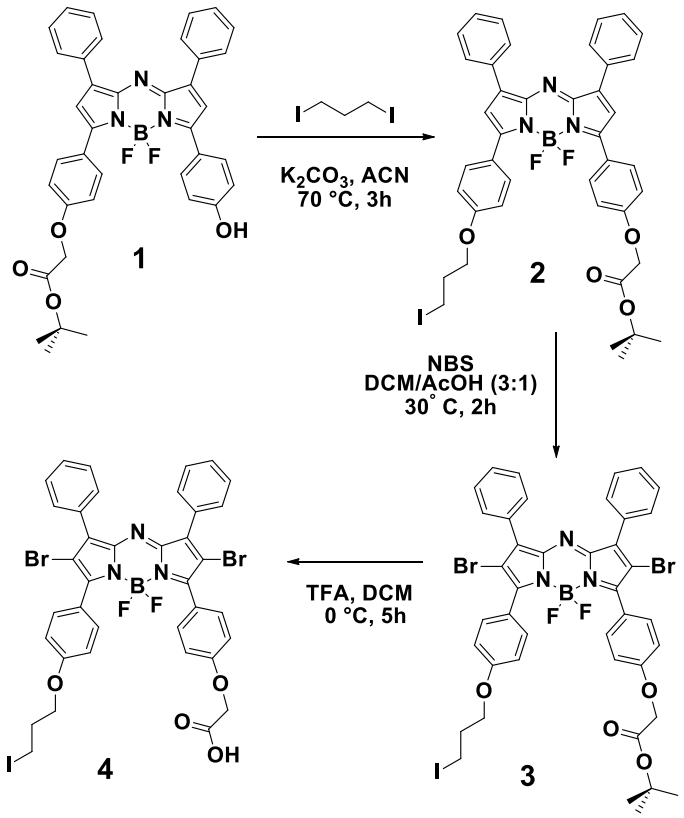

Scheme S1. Synthesis and functionalization of the photosensitizer (PS).

2.1.1 Synthesis of tert-butyl 2-(4-(5,5-difluoro-7-(4-(3-iodopropoxy)phenyl)-1,9-diphenyl-5H-4l4,5l4-dipyrrolo[1,2-c:2',1'-f][1,3,5,2]triazaborinin-3-yl)phenoxy)acetate (PS 2)

Compound **1**, which was obtained via literature procedures,[4b] (2.19 g, 4.04 mmol, 1 eq) was dissolved in dry acetonitrile (15 mL) and K_2CO_3 was added (5.58 g, 40.4 mmol, 10 eq) under vigorous stirring. The mixture was placed in an ice bath, and 1,3-diiodopropane (2.32 mL, 20.2 mmol, 5 eq) was added dropwise. The mixture was refluxed at 70°C for 3 h. The reaction solution was cooled down, filtered and partitioned between DCM (50 mL) and deionized water (3×50 mL). The organic layer was separated and dried over Na_2SO_4, filtrated, and the solvent was evaporated under reduced pressure. Product PS **2** was purified by recrystallization in a DCM: petroleum ether (1:9) mixture to yield dark red metallic crystals (2.38 g, 73%).

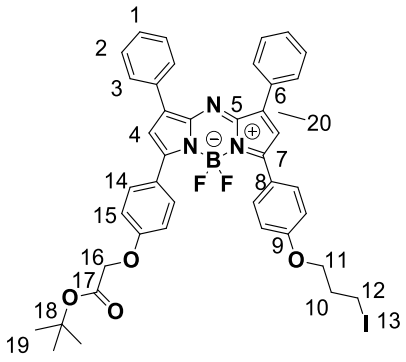

^{1}H NMR (300 MHz, $CDCl_3$): δ (ppm) 8.14 8.01 (m, $8H_{3+14}$), 7.51 7.38 (m, $6H_{1+2}$), 7.08 6.96 (m, $6H_{4+15}$), 4.59 (s, $2H_{16}$), 4.13 (t, *J* = 5.8 Hz, $2H_{11}$), 3.39 (t, *J* = 6.7 Hz, $2H_{12}$), 2.37 2.25 (m, $2H_{10}$), 1.52 (s, $9H_{19}$). ^{11}B (500 MHz, $CDCl_3$): δ (ppm) 1.36 (t, J = 100 Hz, 1B). ^{13}C NMR (500 MHz, $CDCl_3$): δ (ppm) 168 (C_{13}), 161.6 (C_7), 160 (C_9), 132.5 (C_{20}), 129.8 (C_5), 125.3 (C_6), 115 (C_{15}), 83.4 (C_{18}), 67.9 (C_{11}), 66.2 (C_{16}), 33.2 (C_{10}), 28.4 (C_{19}), 2.69 (C_{12}). HRMS (ESI): m/z [+] calculated for $C_{41}H_{37}BF_2IN_3O_4$: 811.1890; found 811.1883.

2.1.2 Synthesis of tert-butyl 2-(4-(2,8-dibromo-5,5-difluoro-7-(4-(3-iodopropoxy)phenyl)-1,9-diphenyl-5H-4l4,5l4-dipyrrolo[1,2-c:2',1'-f][1,3,5,2]triazaborinin-3-yl)phenoxy)acetate (PS 3)

Compound PS **2** (1.133 g, 6.36 mmol, 1 eq) was dissolved in a chloroform:acetic acid (100 mL, 3:1 v/v) mixture and N-bromosuccinimide (2.066 g, 2.54 mmol, 2.5 eq) was added under vigorous stirring in an inert atmosphere (N_2) for 3 h, at 30°C. The reaction mixture was quenched by sodium bicarbonate (10%) solution, and the organic layer was diluted with DCM and washed with deionized water (2×100 mL). The organic layer as dried over Na_2SO_4, filtered and concentrated under reduced pressure. Column chromatography was performed on silica gel (60 Å, 200-400 mesh) by using pure DCM, solvent removal giving dark red metallic crystals (compound PS **3**, 1.77 g, 72%).

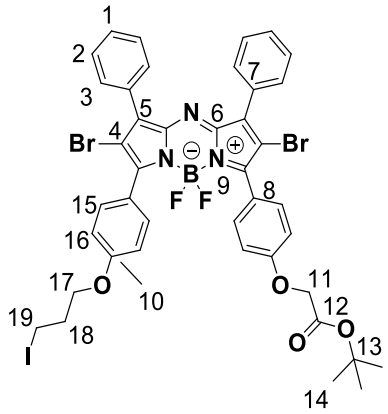

^{1}H NMR (500 MHz, $CDCl_3$) δ (ppm): 7.90 (dd, *J* = 7.4, 2.2 Hz, $4H_3$), 7.81 (d, *J* = 8.8 Hz, $4H_{15}$), 7.50 7.42 (m, $6H_{1+2}$), 7.00 (dd, *J* = 9.0, 2.7 Hz, $4H_{16}$), 4.58 (s, $2H_{11}$), 4.08 (t, *J* = 5.7 Hz, $2H_{17}$), 3.37 (t, *J* = 6.7 Hz, $2H_{19}$), 2.29 (m, $2H_{18}$), 1.53 (s, $9H_{14}$). ^{11}B (500 MHz, $CDCl_3$): δ (ppm): 0.55 (t, J = 85 Hz). ^{13}C NMR (500 MHz, $CDCl_3$): δ (ppm) 168.11 (C_{12}), 161.31 (C_9), 160.46 (C_9), 158.14 (C_{10}), 157.57 (C_{10}), 144.73 (C_5), 142.89 (C_5), 133.00 (C_6), 131.23 (C_{15}), 130.01 (C_{14}), 128.46 (C_{1+2}), 123.08 (C_7), 122.36 (C_8), 114.48 (C_{16}), 83.09 (C_{13}), 67.73 (C_{17}), 66.14(C_{11}), 33.31(C_4), 28.53(C_{14}), 2.9 (C_{19}). HRMS: APCI, calculated for $C_{41}H_{36}BBr_2F_2IN_3O_4$ $[M+H]^+$: m/z 970.0152; found m/z 970.0145.

2.1.3 Synthesis of 2-(4-(2,8-dibromo-5,5-difluoro-7-(4-(3-iodopropoxy)phenyl)-1,9-diphenyl-5H-4l4,5l4-dipyrrolo[1,2-c:2',1'-f][1,3,5,2]triazaborinin-3yl)phenoxy)acetic acid (PS 4)

Compound PS **3** (470 mg, 0.484 mmol) was dissolved in a dichloromethane:TFA mixture (3 mL, 5:1, v/v) at 0°C and stirred for 3 h at room temperature. The solvent was evaporated under reduced pressure and resulted in a dark red product which was recrystallized in a DCM: petroleum ether mixture (1:9, v/v). The obtained pure crystals were filtered and dried under reduced pressure (compound PS **4**, 407 mg, 92%).

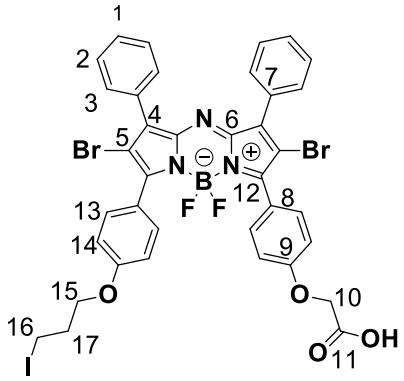

^{1}H NMR (500 MHz, Acetone-d6): δ (ppm) 7.92 (dd, *J* = 8.3 Hz, $4H_3$), 7.76 (dd, *J* = 8.9 Hz, $4H_{13}$), 7.54- 7.48 (m, $6H_{1+2}$), 7.10 (dd, *J* = 9.0 Hz, $4H_{14}$), 4.86 (s, $2H_{10}$), 4.19 (t, *J* = 5.8 Hz, $2H_{15}$), 3.47 (t, *J* = 6.9 Hz, $2H_{16}$), 2.35 2.30 (m, $2H_{17}$). ^{11}B NMR (500 MHz, acetone-d6): δ (ppm) 0.54 (t, *J* = 90 Hz).^{13}C NMR (500 MHz, acetone-d6): δ (ppm) 205.62 (C_{11}), 132.87 (C_{13}), 130.98 (C_3), 130.08 (C_2), 128.55 (C_1), 114.44 (C_{14}), 67.87 (C_{15}), 64.71 (C_{10}), 33.45 (C_{17}), 2.51 (C_{16}). HRMS: APCI, calculated for $C_{37}H_{26}BBr_2F_2N_3O_4$ $[M-H]^-$: m/z 912.9453; found m/z 912.9486.

2.1.4 Heterobifunctional poly(γ-benzyl-l-glutamate) synthesis by ring-opening N-carboxyanhydride polymerization (ROP-NCA)

The cyclic monomer, N-carboxyl-α-amino acid anhydride of γ-benzyl-L-glutamate (NCA-BLG) (2 g, 7.6 mmol), was weighed in a glove box under argon and placed in Schlenk flask. The white NCA-BLG crystals were dissolved in 15 mL anhydrous DMF under argon and placed in a cooling chamber. The initiator, double distilled propargylamine (cryogenic distillation) (9.6 µL, 0.15 mmol), was added dropwise and stirred under static vacuum for 48 h at 0°C. The reaction mixture was concentrated by evaporating the solvent under

reduced pressure and precipitated into cold diethyl ether. The white precipitate was filtered off and dried under high vacuum to afford desired polymer.

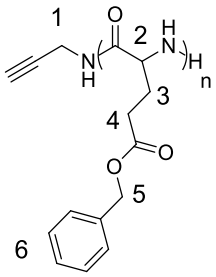

Analysis for $PBLG_{49}$: (DP49, 1.58 g, product yield 95%, primary amine yield ≈93%), SEC (DMF 2.5 mM NH_4PF_6, PEO standards): Mn = 2360 g/mol, Đ = 1.16. ^{1}H NMR (400 MHz, CDCl3/TFA 85/15%): δ (ppm) 7.87–7.85 (d, *J* = 6.7 Hz, 49H, N-H), 7.37–7.27 (m, $250H_6$), 5.17–5.05 (m, $100H_5$), 4.60 (br s, $49H_2$), 4 (m, $2H_1$), 2.47–2.44 (t, *J* = 7.0Hz, $100H_4$), 2.20–1.90 (br m, $100H_3$).

Analysis for $PBLG_{54}$: (DP54, 1.52 g, isolated yield 92%), SEC (DMF 2.5 mM NH_4PF_6, PEO standards): Mn = 3240 g/mol, Đ = 1.14. ^{1}H NMR (400 MHz, CF3COOD (15%)/CDCl3): δ (ppm) 7.69 (d, *J* = 6.9 Hz, 54H, N-H), 7.08-7.17 (m, 270 H_6), 4.88 4.98 (m, $108H_5$), 4.45 (br s, $54H_2$), 3.83 (m, $2H_1$), 2.29 (t, *J* = 7.0 Hz, $108H_4$), 1.94-1.77 (br, $108H_3$).

2.1.5 Monofunctional poly(γ-benzyl-l-glutamate) synthesis by ring-opening N-carboxyanhydride polymerization (ROP-NCA)

N-carboxyl-α-amino acid anhydride of γ-benzyl-L-glutamate (NCA-BLG) (2 g, 7.604 mmol), was weighed in a glove box under argon and placed in Schlenk flask. The white NCA-BLG crystals were dissolved in anhydrous DMF (10 mL) under argon and placed in a cooling chamber (0°C). The initiator, double distilled n-hexylamine (cryogenic distillation) (20 µL, 0.152 mmol), was added dropwise and stirred under static vacuum for 96 h at 0°C. The reaction mixture was concentrated by evaporating the solvent under reduced pressure and precipitated into cold diethyl ether. The white precipitate was filtered off and dried under high vacuum. (DP=53, 1.44 g, 87%, primary amine yield 98%).

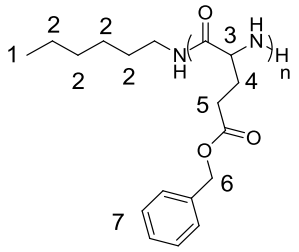

SEC (DMF 2.5 mM NH_4PF_6, PEO standards): Mn = 2860 g/mol, Đ = 1.14. ^{1}H NMR (400 MHz, $CDCl_3$): δ (ppm) 7.72 (d, *J* = 7.0 Hz, 53H, N-H), 7.12 7.22 (m, $265H_7$), 5.03 4.91 (m, $106H_6$), 4.47 (br t, *J* = 10.4 Hz, $53H_3$), 2.32 (t, *J* = 7.0 Hz, $106H_5$), 1.76-2 (m, $106H_4$), 1.15 (br, $8H_2$), 0.75 (t, *J* = 6.8 Hz, $3H_1$).

2.1.6 Peptidic coupling between brominated Aza-BODIPY (PS 4) and poly(γ-benzyl-l-glutamate)

2.1.6.1 Synthesis of PS-$PBLG_{49}$ conjugate

Compound PS **4** (43 mg, 0.05 mmol, 1.5 eq), $PBLG_{49}$ (340 mg, 0.032 mmol) and hydroxybenzotriazole (HOBT, 11 mg, 0.08 mmol, 2.5 eq) were placed in a flask and kept under vacuum for 1 h. 3 mL DCM and 2 mL dimethylacetamide (DMA) were then added while vigorously stirring in an ice bath. The reaction solution was degassed by 3 freeze-pump-thaw cycles, and coupling agent (1-ethyl-3-(3-dimethylaminopropyl) carbodiimide (EDCI, 18 mg, 0.1 mmol, 3 eq) was added. The mixture was stirred for 3 h in an ice bath, then 48 h at room temperature under nitrogen. The solution was diluted with DCM and washed three times with water. The organic layer was dried over Na_2SO_4, filtered and concentrated under reduced pressure. The purification of the conjugate was performed by preparative size exclusion chromatography (SEC, in DCM) on Bio-Beads SX1. Pure conjugate PS-$PBLG_{49}$ was recovered and precipitated into cold diethyl ether. The obtained dark green product was dried under high vacuum to afford 325 mg (88%) of the functionalized polymer. The degree of functionalization was calculated at 92% according to ^{1}H-NMR spectra.

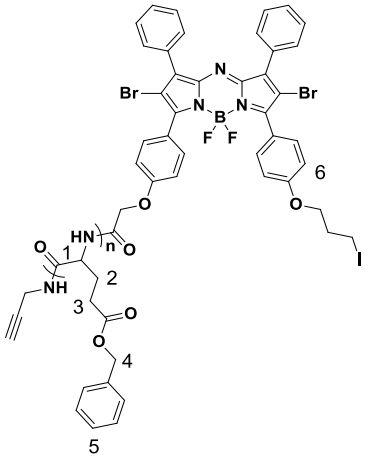

SEC (DMF 2.5 mM NH_4PF_6, PEO standards) Mn = 2760 g/mol, Đ = 1.16. ^{1}H NMR (400 MHz, $CDCl_3$): δ (ppm) 8.25 (br, NH), 7.67-7.81 (m, Ph, BODIPY), 7.17-7.20 (br, 245H_5), 6.82 (d, *J* = 8.6 Hz, 2H_6), 4.95 (s, 100H_4), 3.86 (s, 49H_1), 2.07-2.51 (br, 200H_{2+3}).

2.1.6.2 Synthesis of PS-PBLG$_{53}$ conjugate

Compound PS **4** (71 mg, 0.08 mmol, 1.5 eq), PBLG$_{49}$ (600 mg, 0.052 mmol) and hydroxybenzotriazole (HOBT, 17 mg, 0.13 mmol, 2.5 eq) were placed in a flask and dried under vacuum for 1 h. DCM (3 mL) and dimethylacetamide (2 mL, DMA) were added, while vigorously stirring in an ice bath. The reaction solution was degassed by three freeze-pump-thaw cycles and coupling agent, (1-ethyl-3-(3-dimethylaminopropyl) carbodiimide (EDCI, 30 mg, 0.15 mmol, 3 eq) was added, stirred for 3 h in an ice bath and 48 h at room temperature under nitrogen. The solution was diluted with DCM and washed three times with water. The organic layer was dried over Na_2SO_4, filtered and concentrated under reduced pressure. The purification of the conjugate was performed by preparative size exclusion chromatography (SEC, in DCM) on Bio-Beads SX1. Pure conjugate PS-PBLG$_{53}$ was recovered and precipitated into cold diethyl ether. The obtained dark green product was dried under high vacuum to afford 630 mg (97%) of the functionalized polymer. The degree of functionalization was calculated as 100% according to ^{1}H-NMR spectra.

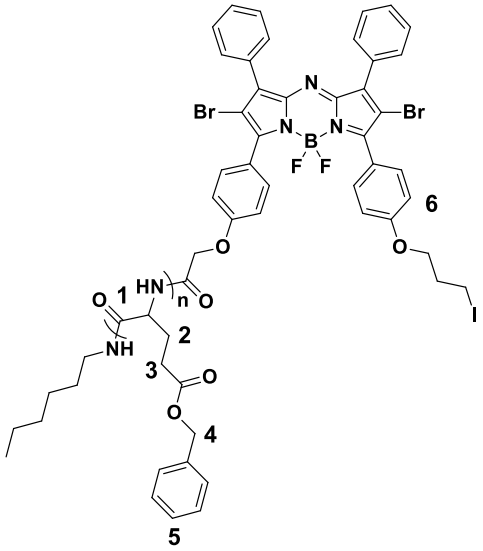

SEC (DMF 2.5 mM NH_4PF_6, PEO standards) Mn = 3230 g/mol, Đ = 1.18. ^{1}H NMR (400 MHz, $CDCl_3$): δ (ppm) 8.26 (br s, NH), 7.68-7.80 (m, Ph, Aza-BODIPY), 7.32 7.05 (br m, 265H_5), 6.84 (d, *J* = 8.6Hz, 2H_6), 4.96 (br s, 106H_4), 3.86 (br s, 53H_1), 2.05-2.50 (br, 212H_{2+3}).

2.1.7 Azide functionalization of the chain end of PS-PBLG$_{53}$ conjugate

PS-PBLG$_{53}$ (659 mg, 0.057 mmol, 1 eq) was dissolved in THF (5 mL). Azidotrimethylsilane ($TMSN_3$, 22 µL, 0.17 mmol, 3 eq) and tetrabutylammonium fluoride (TBAF, 33 µL, 0.13 mmol, 2 eq) were added at 0°C, and the mixture was stirred at room temperature for 24 h under nitrogen. The reaction mixture was diluted with THF and partitioned between DCM (50 mL) and deionized water (4 x 50 mL). The organic layer was separated, dried over Na_2SO_4, filtered, concentrated under reduced pressure, and precipitated into cold diethyl ether. The resulting dark green precipitate was filtered and dried under high vacuum (574 mg, 87%).

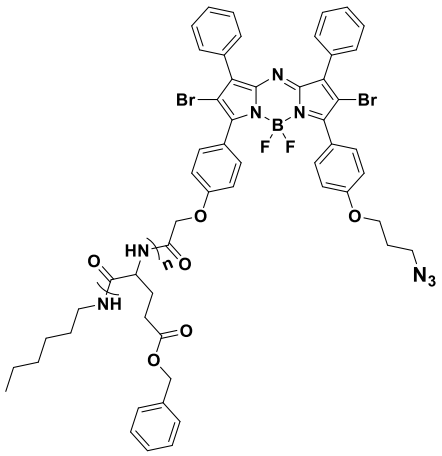

IR (ATR-FTIR) υ_{max} 3290, 3031, 2954, 2190, 1734, 1652, 1548, 1167, 772, 699 cm^{-1}

2.1.8 Amphiphilic block copolymer synthesis by CuAAC click reaction

2.1.8.1. Amphiphilic PS-PBLG-*b*-PEG type (SPG) block copolymer

$PEG\text{-}N_3$ (Mn = 5000 g/mol or 2000 g/mol, 1.5 eq), PBLG (1 eq) and tris(benzyltriazolylmethyl)amine (TBTA, 1 eq) were dissolved in dry DCM under nitrogen and degassed via 3 freeze-pump-thaw cycles. CuBr (1 eq) was then added and the solution was degassed one more time and stirred at ambient temperature for 24 h under nitrogen. The solution was filtered and partitioned between EDTA (400 mg/L) solution and DCM. The organic phase was separated, dried over $MgSO_4$ and concentrated. The crude product was purified by column chromatography on silica gel (60 Å, 200-400 mesh) by using a DCM:MeOH (9:1, v/v) mixture as eluent. The pure block copolymer fraction was concentrated under reduced pressure, precipitated into cold diethyl ether and filtered. The green precipitate was dried, washed with deionized water several times and lyophilized.

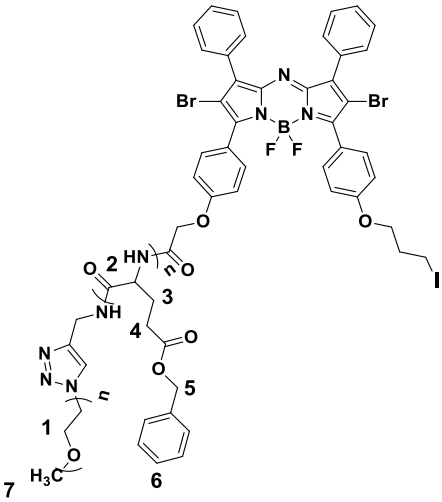

Analysis for $PS\text{-}PBLG_{49}\text{-}b\text{-}PEG_{45}$ (Starting $PS\text{-}PBLG_{49}$ 150 mg, yield of the block copolymer 168 mg, 94% (click reaction yield calculated from ^1H NMR 100%)): SEC (DMF 2.5 mM NH_4PF_6, PEO standards) Mn = 3930 g/mol, Đ = 1.19. ^1H NMR (400 MHz, $CDCl_3$): δ (ppm) 8.26 (br, NH), 7.21 (br, $255H_6$), 4.96 (br, $100H_5$), 3.85 (br, $49H_2$), 3.58 (m, $182H_1$), 3.31 (s, $3H_7$), 2.25 (br, $207H_{3+4}$).

2.1.8.2 Amphiphilic PBLG-PS-*b*-PEG type (PSG) block copolymer synthesis

PEG-alkyne (Mn = 2000 g/mol, 1 eq), PBLG (1 eq) and tris(benzyltriazolylmethyl) amine (TBTA, 1 eq) were dissolved in dry DCM under nitrogen and degassed via 3 freeze-thaw cycles. CuBr (1 eq) was then added and the solution was degassed one more time and stirred at ambient temperature for 24 h under nitrogen. The solution was filtrated and partitioned between EDTA (400 mg/L) solution and DCM. The organic phase was separated, dried over $MgSO_4$ and concentrated. Crude product was purified by column chromatography on silica gel (60 Å, 200-400 mesh) by using a DCM:MeOH (9:1, v/v) mixture as eluent. The pure block copolymer fraction was concentrated under reduced pressure, precipitated in cold diethyl ether and filtered. The green precipitate was dried, washed several times with deionized water and lyophilized.

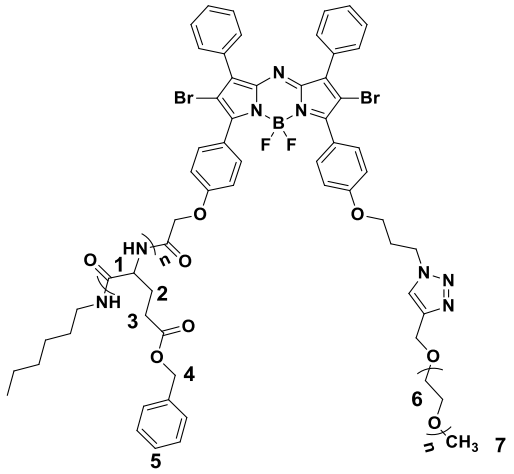

Analysis for $PBLG_{53}$-PS-*b*-PEG_{45} (Starting $PBLG_{53}$-PS 280 mg, isolated yield of the block copolymer 198 mg, 61% (click reaction yield calculated from ^1H NMR 72%)): SEC (DMF 2.5 mM NH_4PF_6, PEO standards) Mn = 4940 g/mol, Đ = 1.22. ^1H NMR (400 MHz, $CDCl_3$): δ (ppm) 8.28 (br, NH), 7.18 (br, $265H_5$), 4.96 (br, $109H_4$), 3.86 (br, $53H_1$), 3.57 (m, $189H_6$), 3.31 (s, $3H_7$), 2.27 (br, $236H_{2+3}$).

2.1.8.3 PS free PBLG-*b*-PEG type block copolymer synthesis by Cu(II) catalyzed click reaction

PEG-N_3 (Mn = 2000 g/mol, 1.5 eq) and $PBLG_{54}$ (1 eq) were dissolved in DMSO at 30°C. Sodium ascorbate (3.5 eq) was added under vigorous stirring and followed by $CuSO_4$ (2 eq) addition. The solution was stirred at 30°C for 48 h under nitrogen. The solution was diluted with DCM and washed five times with EDTA (400 mg/L) solution and twice with deionized water. The organic phase was separated, dried over $MgSO_4$ and concentrated under reduced pressure. The concentrated polymer solution in DCM was precipitated into cold diethyl ether and filtered. The white precipitate was dried, washed with deionized water and centrifuged several times to remove excess PEG and finally dried by lyophilization.

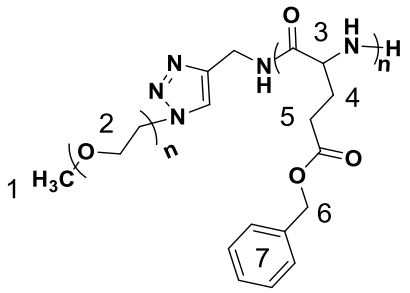

Analysis for $PBLG_{54}$-*b*-PEG_{45} (Starting $PBLG_{54}$ 500 mg, yield of the block copolymer 531 mg, 91% (click reaction yield calculated from ^1H NMR is 100%)): SEC (DMF 2.5 mM NH_4PF_6, PEO standards) Mn = 5520 g/mol, Đ = 1.15. ^1H NMR (400 MHz, $CDCl_3$): δ (ppm) 8.26 (br, NH), 7.18 (br, $270H_7$), 4.96 (br, $108H_6$), 3.86 (br, $54H_3$), 3.57 (m, $182H_2$), 3.31 (s, $3H_1$), 2.05-2.53 (br, $216H_{4+5}$).

2.2 NMR spectra

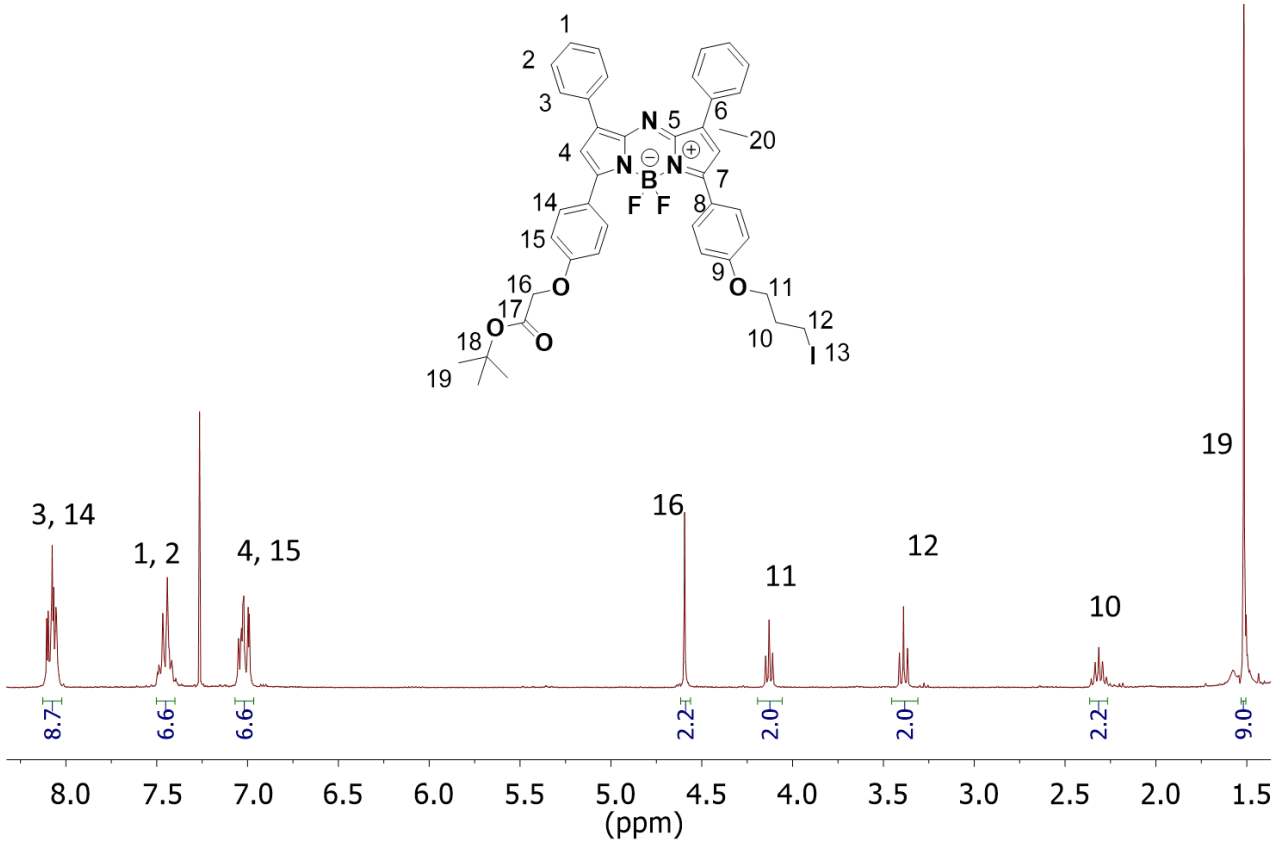

Figure S3. ^{1}H-NMR spectrum of compound PS **2** (300 MHz, $CDCl_3$)

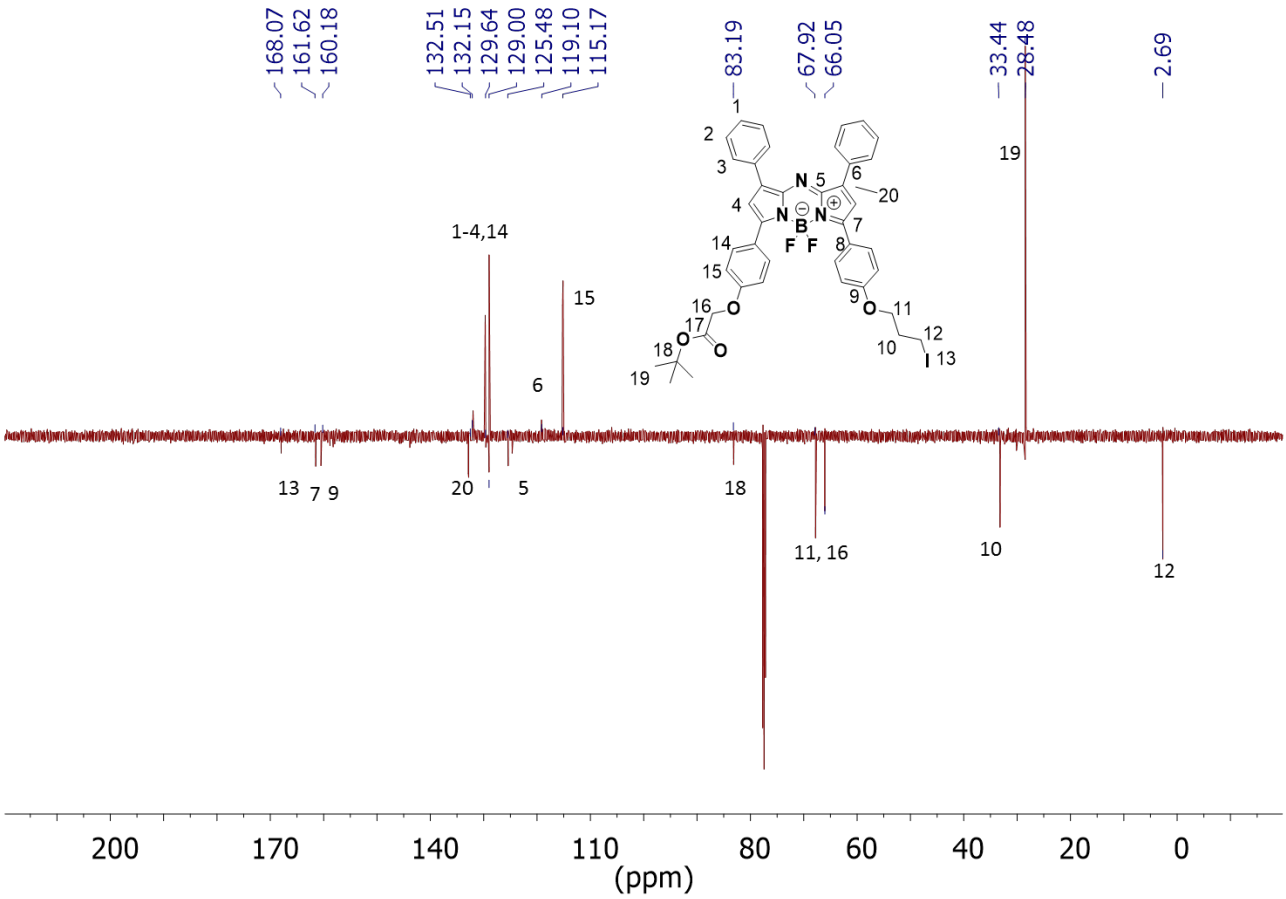

Figure S4. ^{13}C-NMR spectrum of compound PS **2** (DEPT135, 500 MHz, $CDCl_3$).

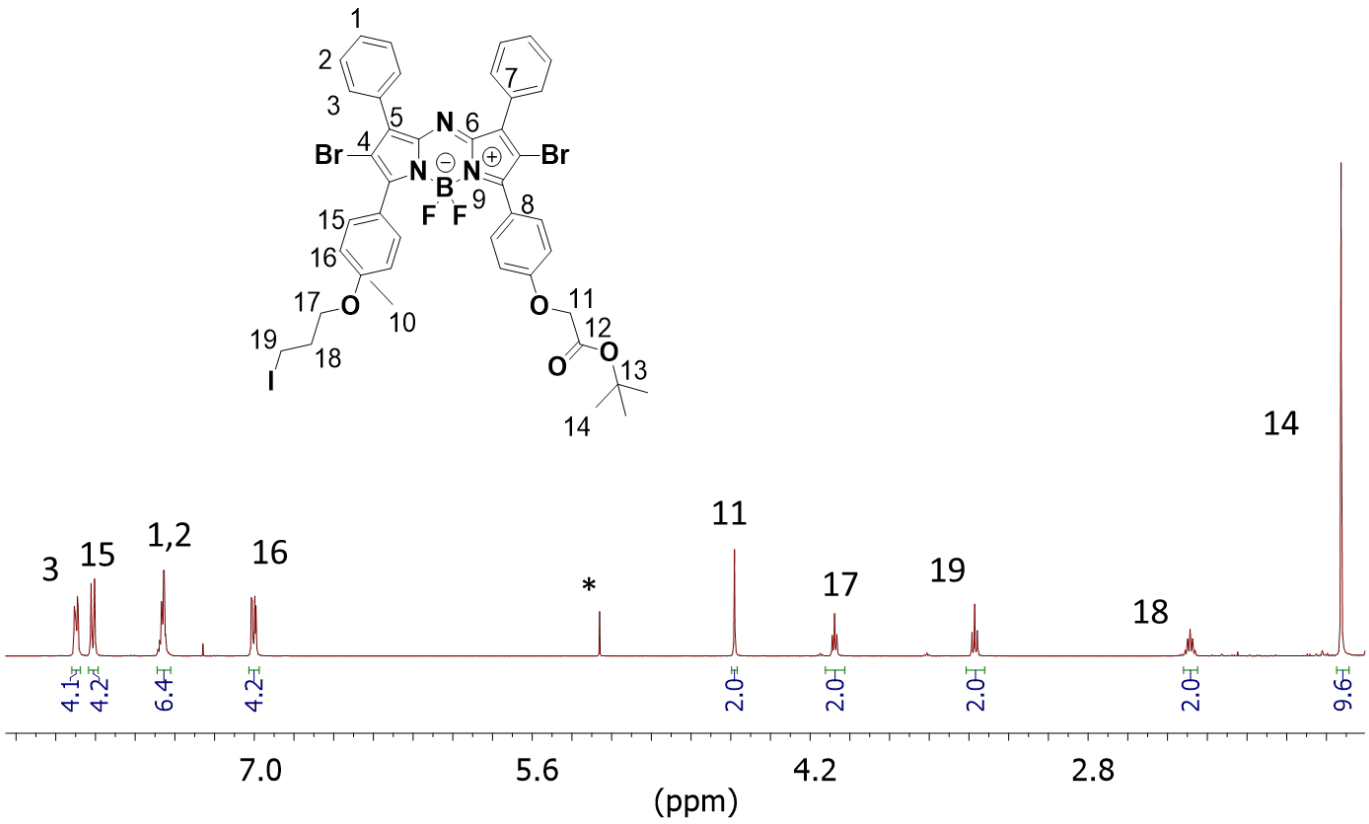

Figure S5. ^{1}H-NMR spectrum of compound PS **3** (500 MHz, $CDCl_3$)

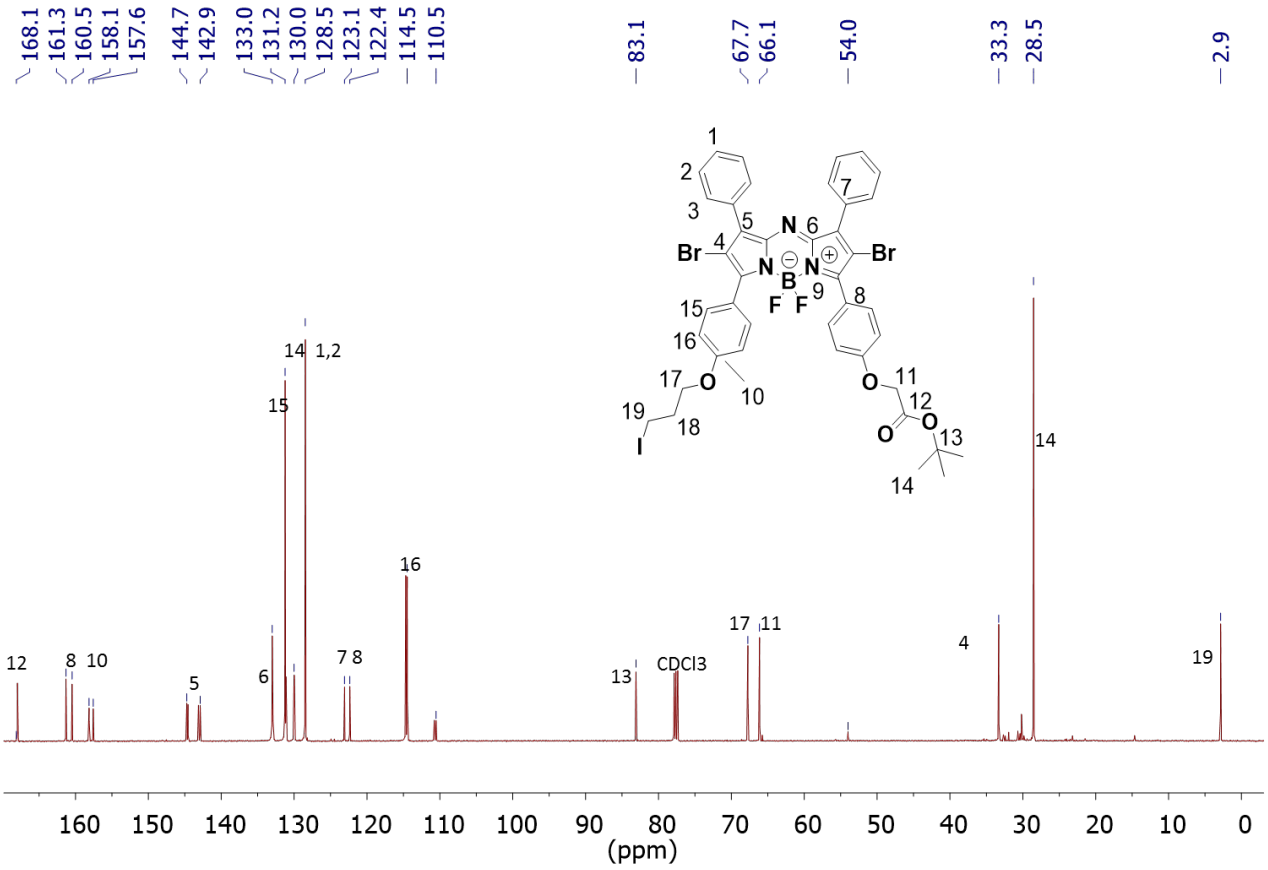

Figure S6. ^{13}C-NMR spectrum of compound PS **3** (500 MHz, $CDCl_3$).

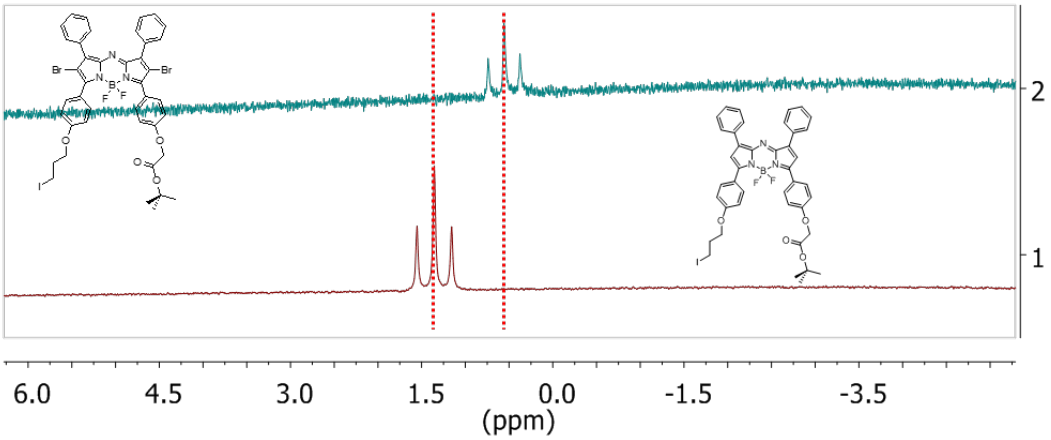

Figure S7. ^{11}B-NMR spectrum of (1) compound PS **3**, (2) compound PS **4** (500 MHz, $CDCl_3$).

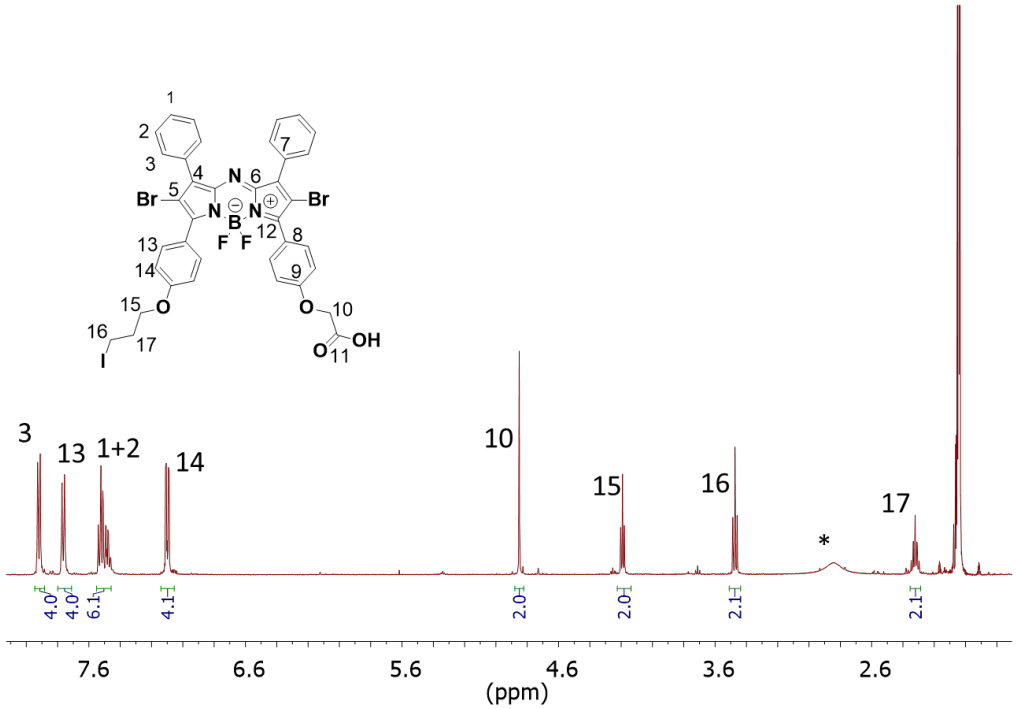

Figure S8. ^{1}H-NMR spectrum of compound PS **4** (500 MHz, acetone-d6).

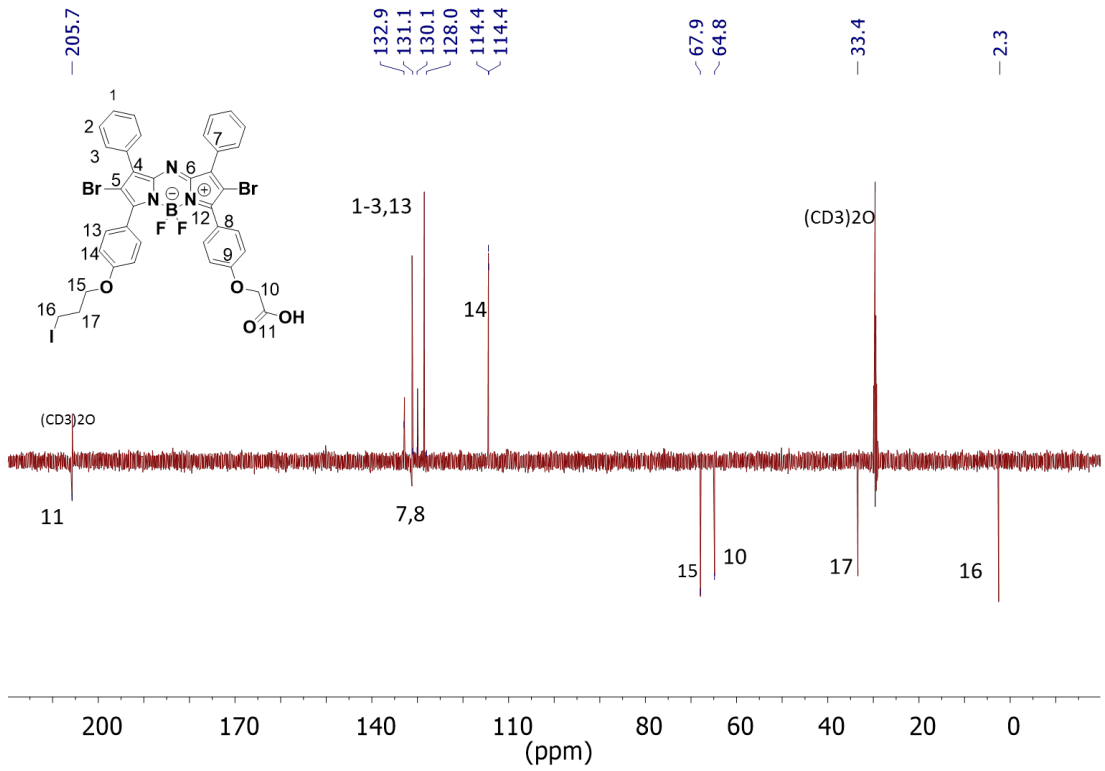

Figure S9. ^{13}C-NMR spectrum of compound PS **4** (DEPT135, 500 MHz, acetone-d6).

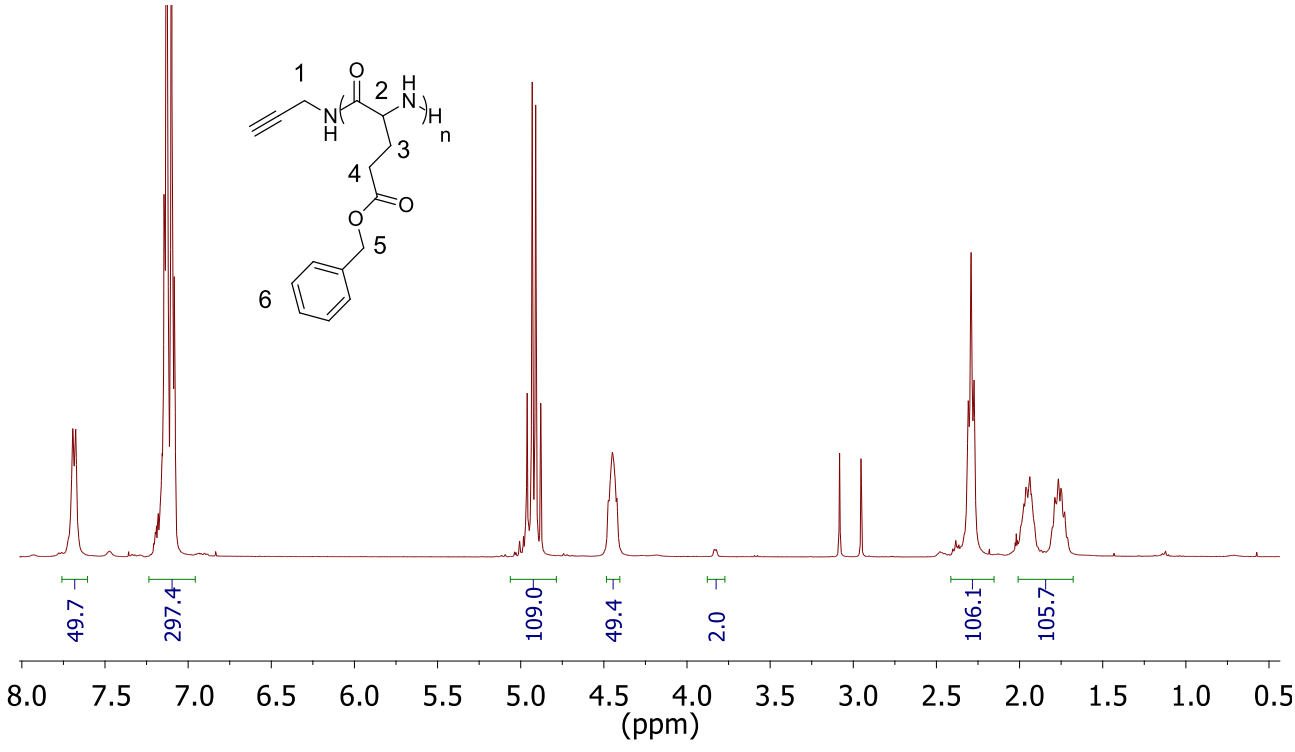

Figure S10. ^{1}H-NMR spectrum of bi-functionalized $PBLG_{49}$ (400 MHz, TFA/$CDCl_3$, * = DMF).

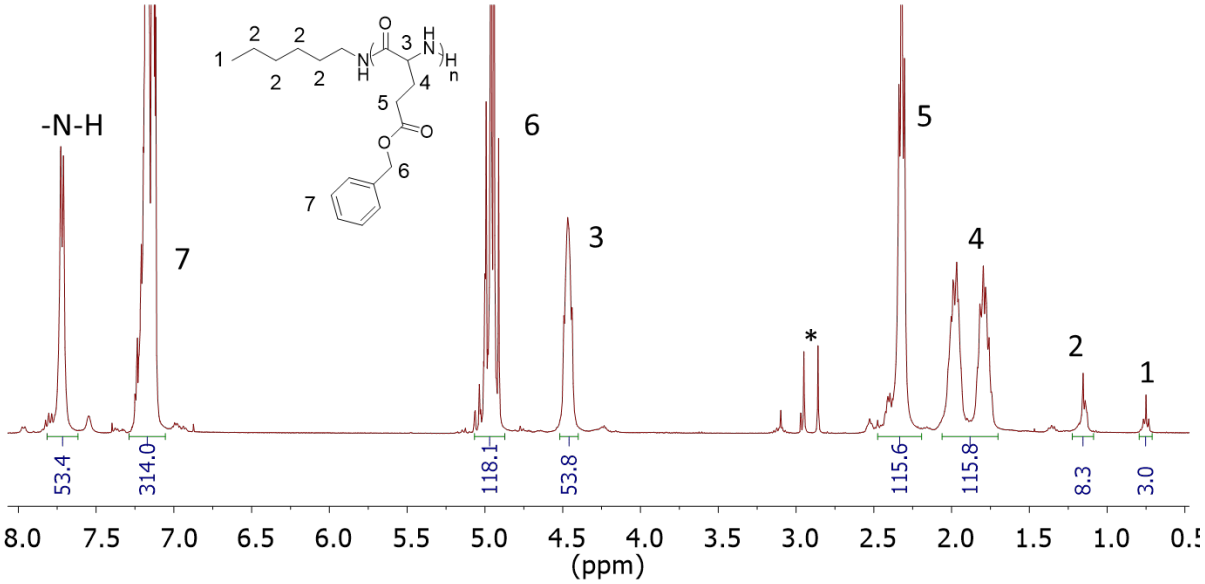

Figure S11. ^{1}H-NMR spectrum of mono-functionalized $PBLG_{53}$ (400 MHz, TFA/$CDCl_3$, * = DMF).

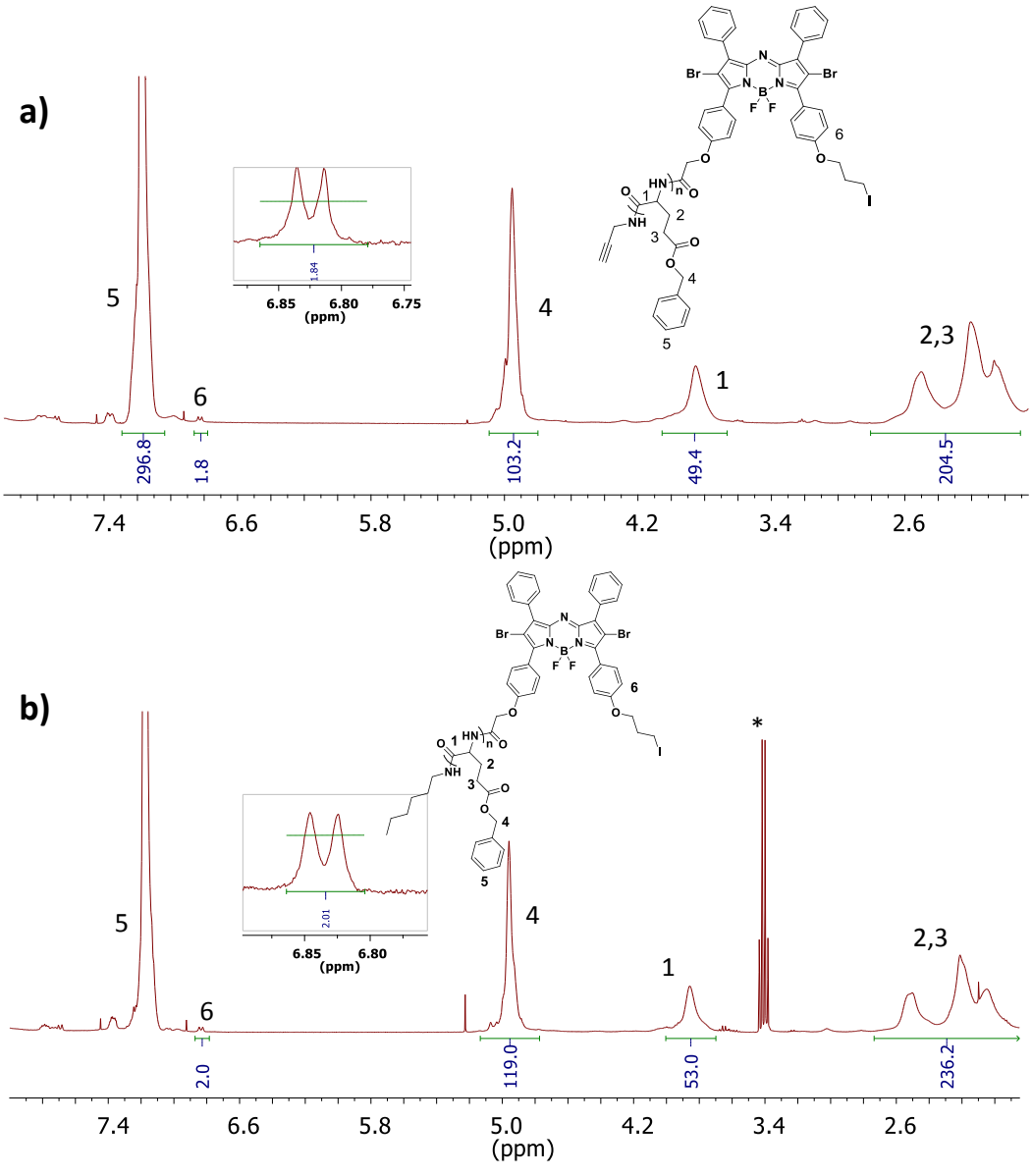

Figure S12. ^{1}H-NMR spectra of a) $PBLG_{49}$-PS conjugate, b) $PBLG_{53}$-PS conjugate (400 MHz, $CDCl_3$, * = Et_2O).

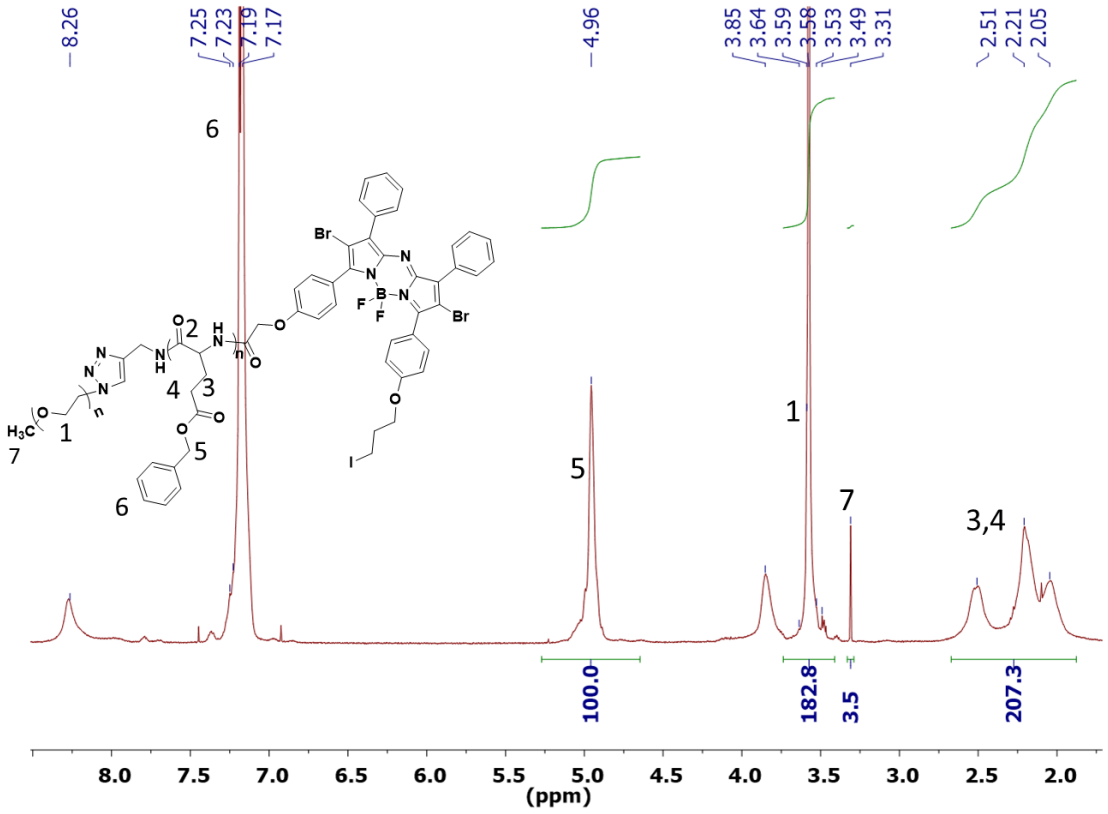

Figure S13. ^{1}H NMR spectrum of PS-PBLG$_{49}$-*b*-PEG$_{45}$ block copolymer (400 MHz, $CDCl_3$).

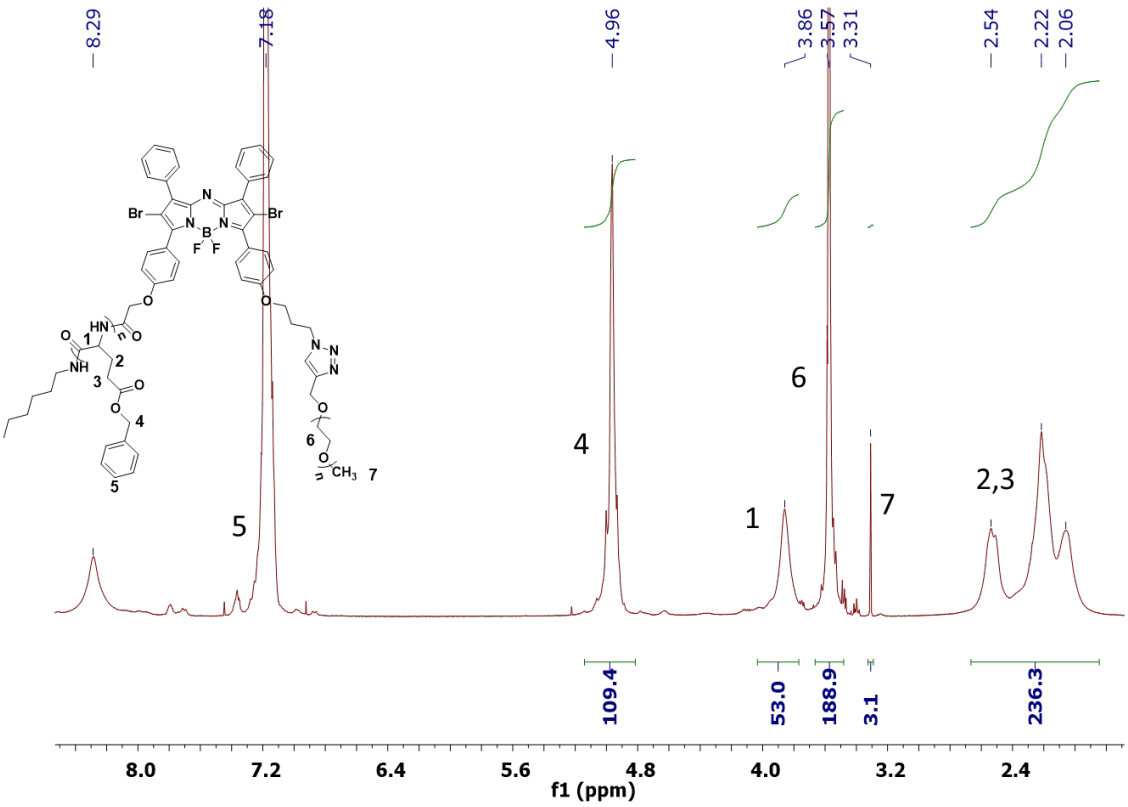

Figure S14. ^{1}H NMR spectrum of PBLG$_{53}$-PS-*b*-PEG$_{45}$ block copolymer (400 MHz, $CDCl_3$).

2.3 Mass spectra.

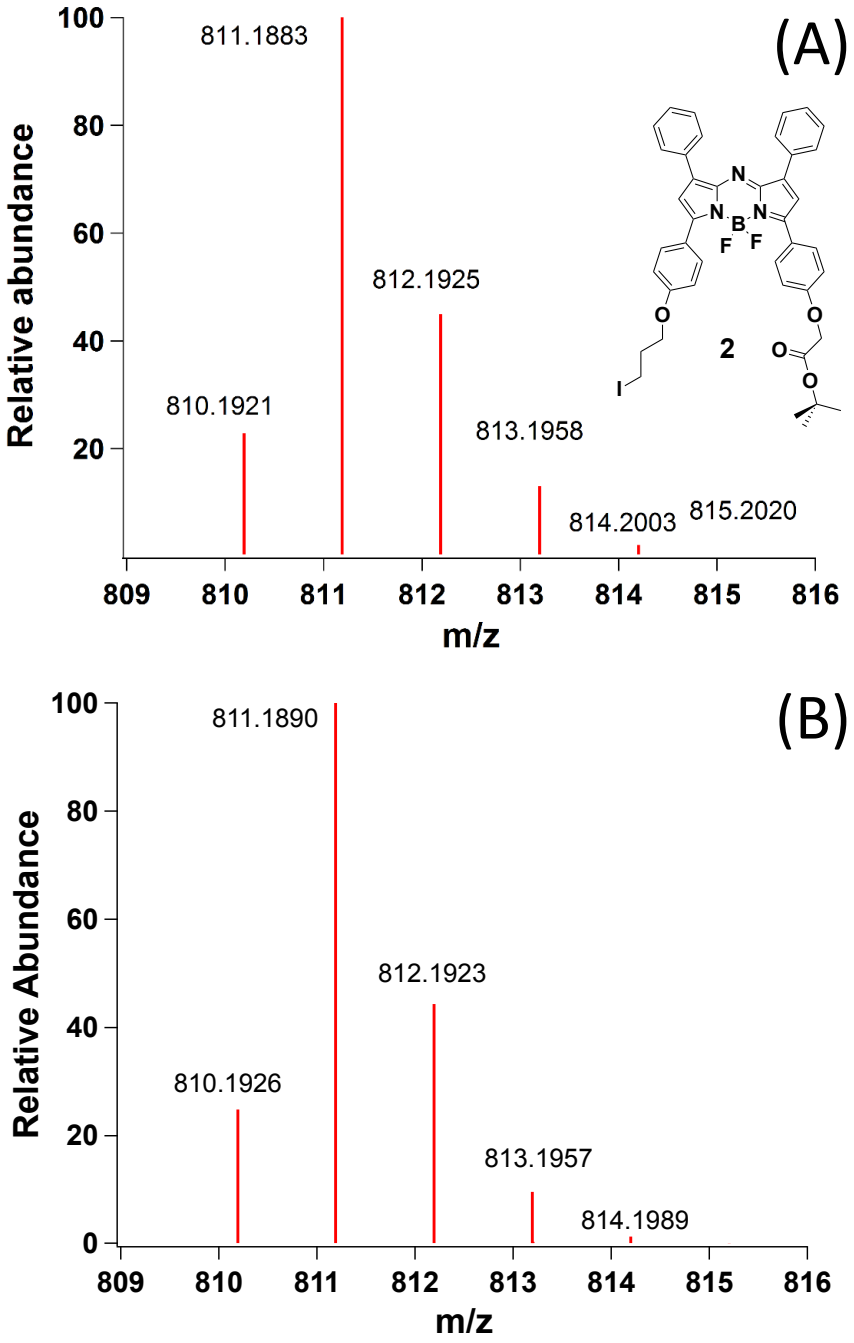

Figure S15. Mass spectroscopy result of compound PS **2** a) experimental isotopic mass distribution obtained from ESI mass spectroscopy measurement b) theoretical prediction.

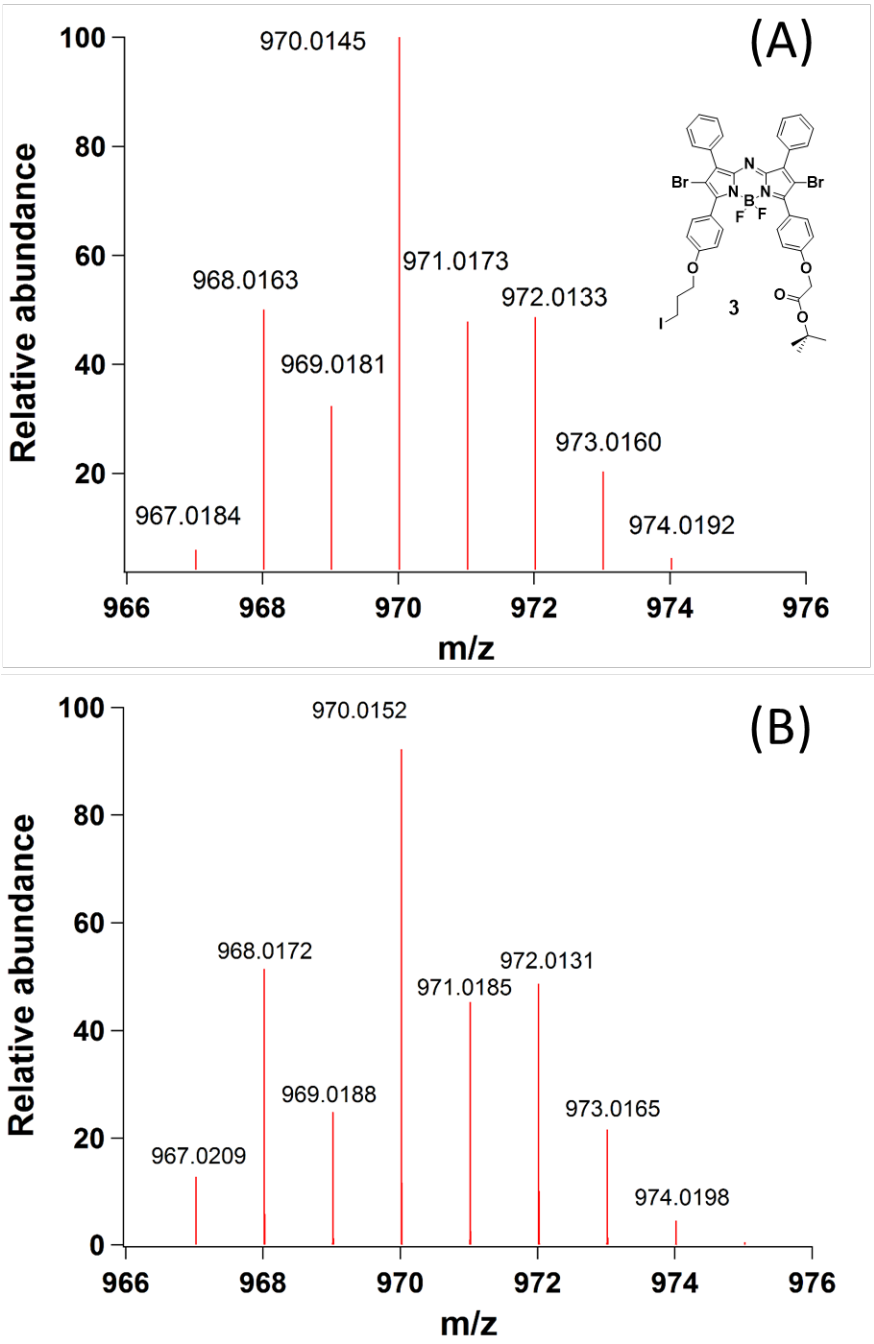

Figure S16. Mass spectroscopy result of compound PS **3** a) experimental isotopic mass distribution obtained from APCI $[M+H]^+$ mass spectroscopy measurement b) theoretical prediction.

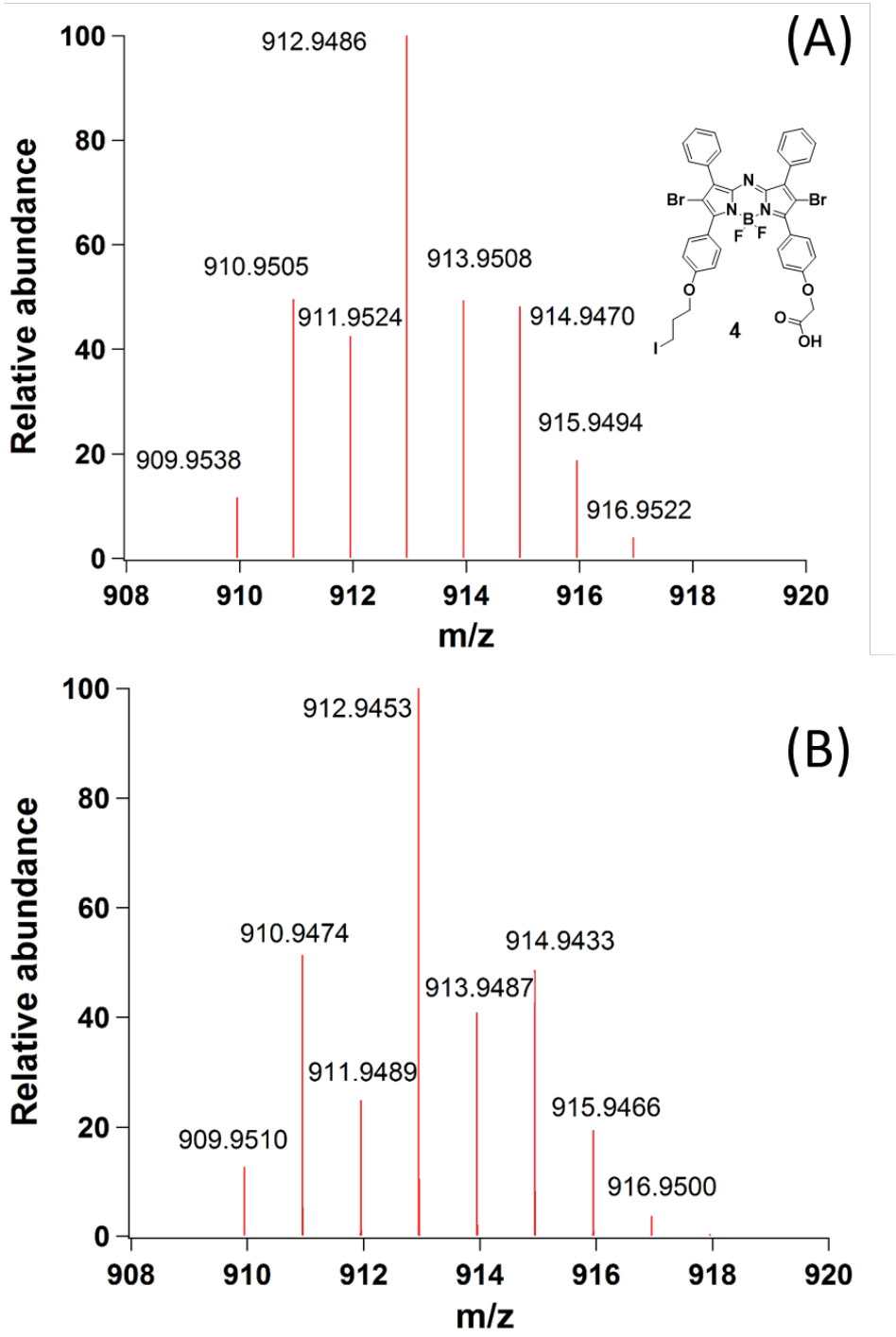

Figure S17. Mass spectroscopy result of compound PS **4** a) experimental isotopic mass distribution obtained from APCI $[M-H]^-$ mass spectroscopy measurement b) theoretical prediction.

2.4 SEC chromatograms

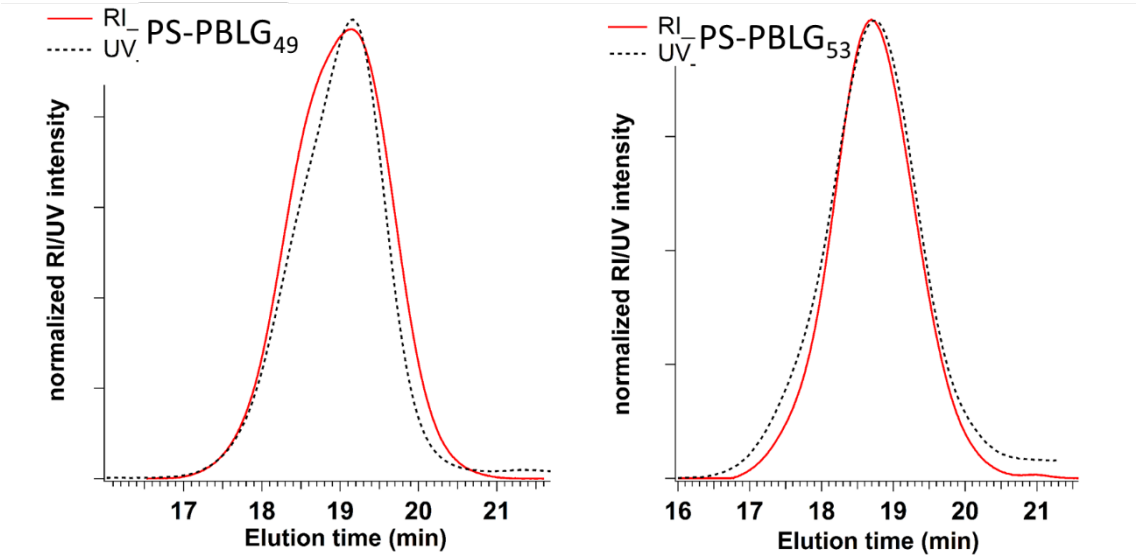

Figure S18. SEC chromatograms for $PBLG_{49}$-PS and $PBLG_{53}$-PS conjugates (DMF 2.5 mM of NH_4PF_6, PEO standards).

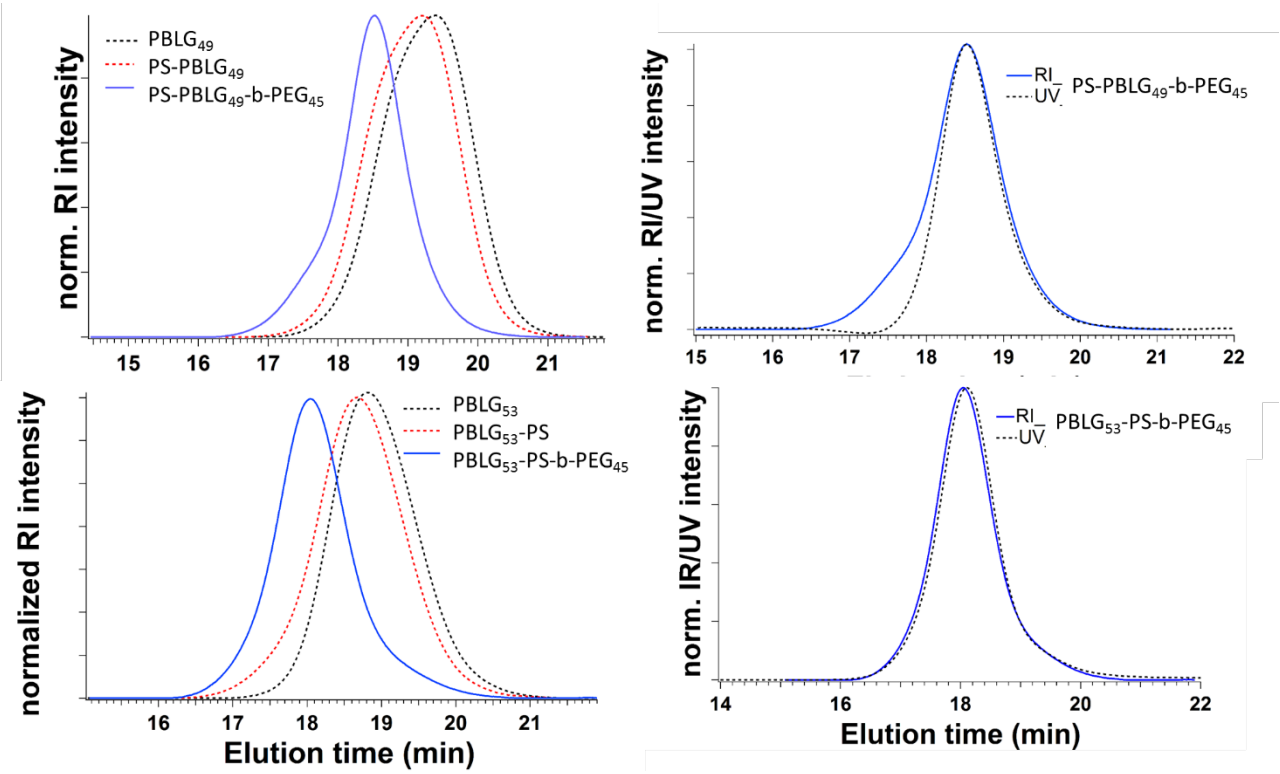

Figure S19. SEC chromatograms of $PBLG_{49}$, $PBLG_{49}$-PS and PS-$PBLG_{49}$-*b*-PEG_{45} polymers $PBLG_{53}$, $PBLG_{53}$-PS and $PBLG_{53}$-PS-*b*-PEG_{45} (DMF 2.5 mM of NH_4PF_6, PEO standards).

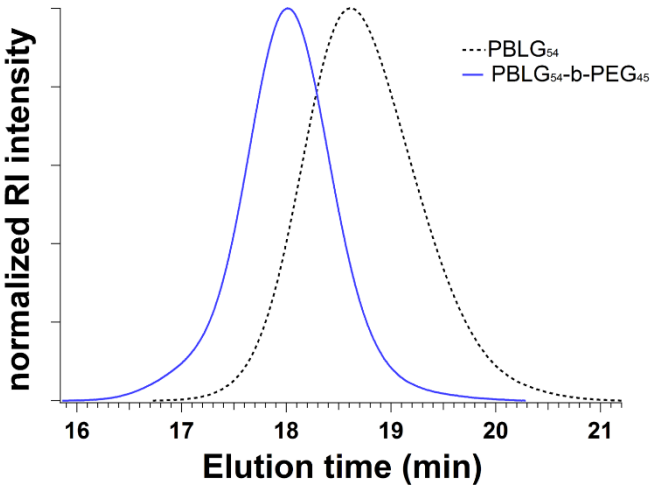

Figure S20. SEC chromatogram of $PBLG_{54}$ and $PBLG_{54}$-*b*-PEG_{45} polymers (DMF 2.5 mM of NH_4PF_6, PEO standards).

2.5 Stability of the vesicles in the presence of cell medium

The stability of the nanocarriers was evaluated in the presence of cell medium (MEM alpha, GlutaMAX(TM)). It is known that a long circulation lifetime of the particles in blood stream is important for EPR effect, to have internalization of a sufficient amount of particles in the tumor site.[5] However, the nanoparticles may form aggregates in the blood stream due to the protein adsorption, which will eventually decrease the efficacy of targeting and of the therapy. Many experimental results from the literature proved that nanomaterials with a PEG corona have stealth property. They can thus escape macrophage recognition and protein or cell adsorption.[6] To test this phenomenon for our nanocarriers we added 10% (v/v) of cell medium (MEM alpha, GlutaMAX(TM)) into 1 g/L nanocarrier solutions and the size was measured at 25°C with time. No aggregate formation was observed under those conditions nor visible precipitate formation. Only a second population at small sizes was observed in the size distribution histogram, which could be due to proteins in the cell medium. To check this we measured the size distribution of proteins in the cell medium by mixing 10% of it with pure Milli-Q water and indeed observed 12 nm size particles that correspond to the small size population in the copolymer MEM solutions. Moreover, to evaluate the stability of the nanocarriers at body temperature we heated the solution up to 37°C and kept it for 12 h. Even after high temperature and longer incubation time no visible aggregate formation was observed in the solutions which confirms the stability of the nanocarriers in the presence of proteins.

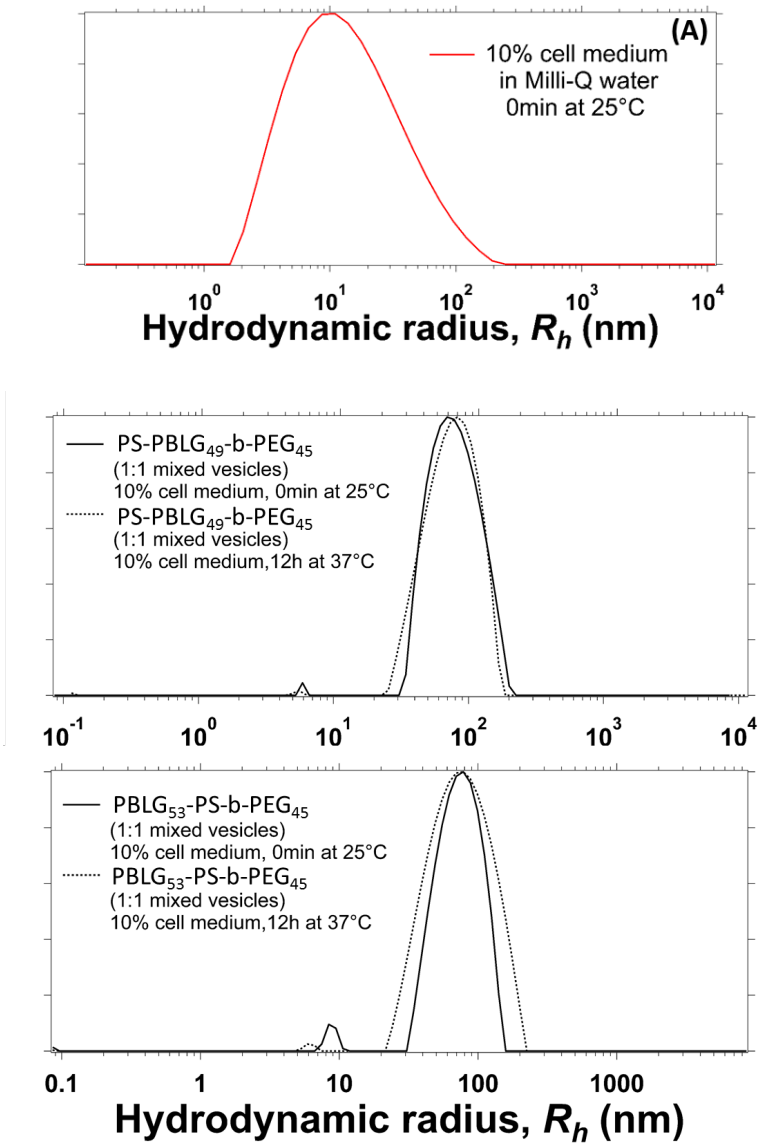

Figure S21. Intensity weighted size distribution diagram obtained by DLS of the (A) 10% (v/v) cell medium (MEM alpha, GlutaMAX(TM)) mixed Milli-Q water (B) and (C) nanocarriers in the presence of 10% (v/v) cell medium (MEM alpha, GlutaMAX(TM)) at 25°C and 37°C.

2.6 Photophysical characterization

Table S1. Overall results from photophysical characterization

	λ_{abs} (nm)	λ_{em} (nm)	Φ_F	τ (ns)	ε [$M^{-1}\cdot cm^{-1}$]	Φ_T	Φ_Δ DCM
PS **2**	689	719	0.36	2.4	83900		
PS **3**	675	712	0.08	0.59(41%), 1.02(59%)	71700	0.57	0.66
PS **4**	676	718	0.07	0.6	69300	0.60	
PS-PBLG$_{53}$	675	712	0.08	0.62(42%), 1.73(58%)	46300	0.58	
PS-PBLG$_{49}$	671	707	0.06	0.41(65%), 1.26(35%)	40200	0.62	
PBLG$_{53}$-PS-*b*-PEG$_{45}$ (P**S**G)	677	712	0.11	0.65(43%), 2.01(57%)	23700	0.50	0.53
PS-PBLG$_{49}$-*b*-PEG$_{45}$ (**S**PG)	672	707	0.06	0.49(40%), 1.6(60%)	23900	0.60	0.43

λ_{abs} absorption maxima, λ_{em} emission maxima, τ fluorescence lifetime, ε extinction coefficient, Φ is quantum yield of F- fluorescence, T- triplet state and Δ-singlet oxygen

2.6.1 Fluorescence quantum yield measurements

The relative fluorescence quantum yields (Φ_F) were determined by the optically dilute method using Aza-BODIPY **5** (BF_2 chelate of [5-(4-methoxyphenyl)-3-phenyl-1H-pyrrol-2-yl]-[5-(4-methoxyphenyl)-3-phenylpyrrol-2-ylidene] amine, Φ_F=0.35 in THF)[2a,4a] in THF as standard.

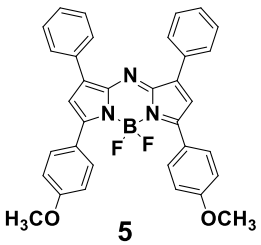

5

The absorptions of the standard and the samples were adjusted to less than 0.1 O.D. at excitation wavelength and Φ_F calculated using equation 1.

$$\Phi_x = \Phi_{st} \times \left(\frac{I_x}{I_{st}}\right) \times \left(\frac{F_{st}}{F_x}\right) \times \left(\frac{\eta_x^2}{\eta_{st}^2}\right) \quad (1)$$

Where Φ_x is the fluorescence quantum yield of the sample, Φ_{st} is the fluorescence quantum yield of the reference compound, I is the integrated emission intensity, F is the optical density at the irradiation wavelength and η is the refractive index of the solvent.

The absolute fluorescence quantum yields (Φ_F) of the nanocarriers in Milli-Q water have been determined by using an integrating sphere (diameter of 100 mm), which provides a reflectance >99% over 400-1500 nm range (>95% within 250-2500 nm). The concentrated micelle solutions (2 mg/mL) were prepared and fluorescence signals were detected IN and OUT of the beam in the cylindrical quartz cuvette (8 mm diameter) which is mounted on a Teflon support inside the sphere. The measurement was performed with and without the sample (rotating the holder by 180°), and to reduce the error an average of 15 measurements have been taken and final Φ_F calculated form equations 2 and 3 which were developed by Mello and coworkers.[7]

$$\Phi_F = \frac{E_{in}(\lambda) - (1-\alpha)E_{out}(\lambda)}{X_{empty}(\lambda)\alpha} ND \quad (2)$$

$$\alpha = \frac{X_{out}(\lambda) - X_{in}(\lambda)}{X_{out}(\lambda)} \quad (3)$$

Where, $E_{in}(\lambda)$ and $E_{out}(\lambda)$ are the integrated luminescence in "IN" and "Out" configuration and α is an absorption of the sample. $X_{empty}(\lambda)$, $X_{in}(\lambda)$, $X_{out}(\lambda)$, integrated excitation of empty sphere, with sample in "IN" configuration and in "OUT" configuration, respectively.

Table S2: Absorption maxima and fluorescence wavelengths of non-brominated, brominated and deprotected Aza-BODIPYs.

	λ_{abs} (nm)		λ_{em} (nm)	
compounds	THF	DCM	THF	DCM
PS 2	689	683	719	715
PS 3	675	674	712	720
PS 4	676	670	718	709

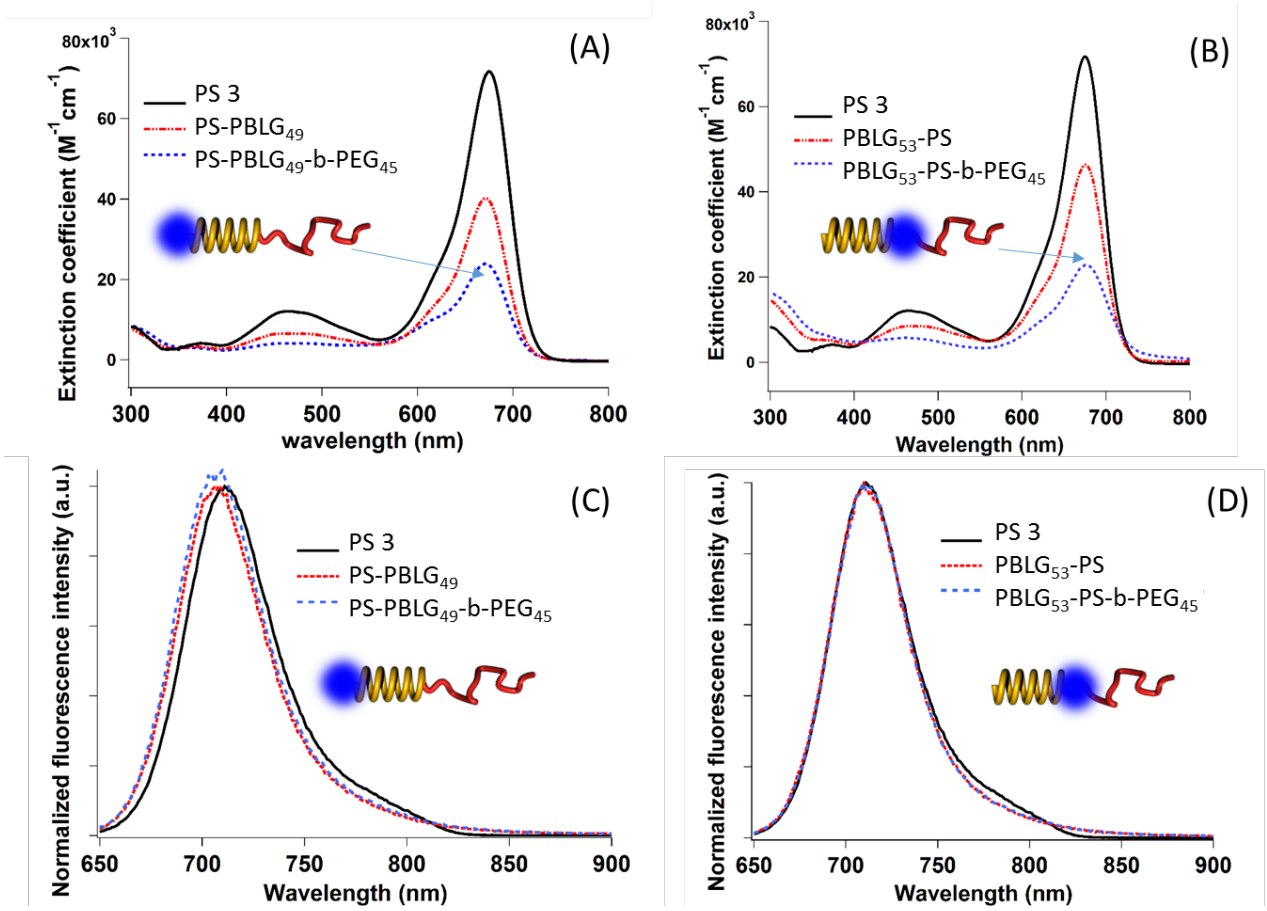

Figure S22. Overlaid absorption of (A) PS **3**, PS-PBLG$_{49}$ and PS-PBLG-*b*-PEG type block copolymers (B) PS **3**, PBLG$_{53}$-PS-N$_3$ and PBLG-PS-*b*-PEG type block copolymers; fluorescence of (C) PS **3**, PS-PBLG$_{49}$ and PS-PBLG-*b*-PEG type block copolymers (D) PS **3**, PBLG$_{53}$-PS-N$_3$ and PBLG-PS-*b*-PEG type block copolymers (λ_{ex} = 630 nm in THF).

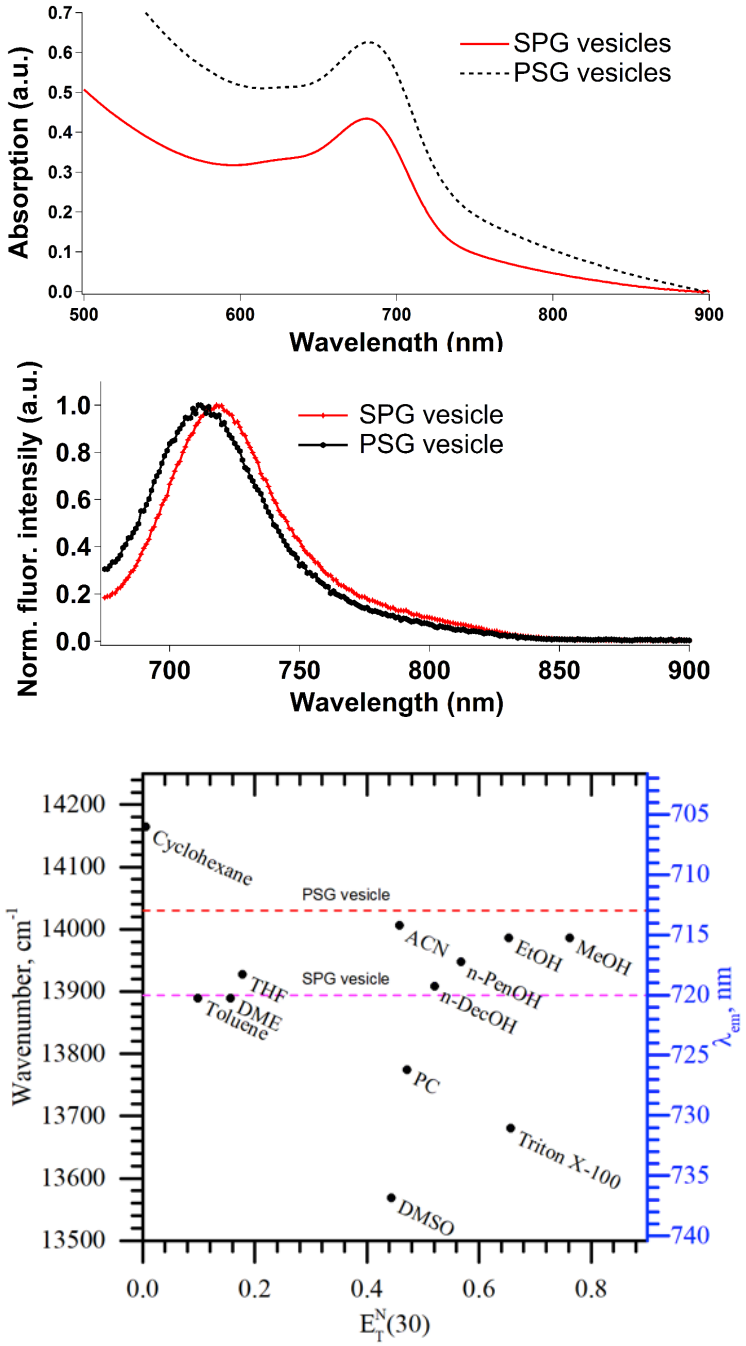

Figure S23. Upper panel: Overlaid UV-vis spectra and fluorescence spectra of vesicles in water (λ_{exc}= 650 nm). Lower panel: Fluorescence emission maxima of benchmark AzaBODIPY **5** in solvents of varying polarity compared with that obtained for **PSG** and **SPG** vesicles.

2.6.2 TRABS and luminescence lifetime measurements

The transient absorbance (TRABS) measurements were performed with a sub-nanosecond set-up (Figure S1) on degassed samples. The samples were dissolved in distilled THF and the absorption band of the samples at excitation wavelength (630 nm) adjusted to 1 O.D. The solutions were degassed by multiple freeze-pump-thaw cycles before the measurements and blowtorch sealed in quartz cells. Fluorescence lifetimes were determined in dilute solutions by time-resolved fluorescence spectroscopy using sub-nanosecond set-up (Figure S1), exciting samples at 600 nm (PYI) and 405 nm (NCS). The data analysis was done using a home written LabVIEW program.

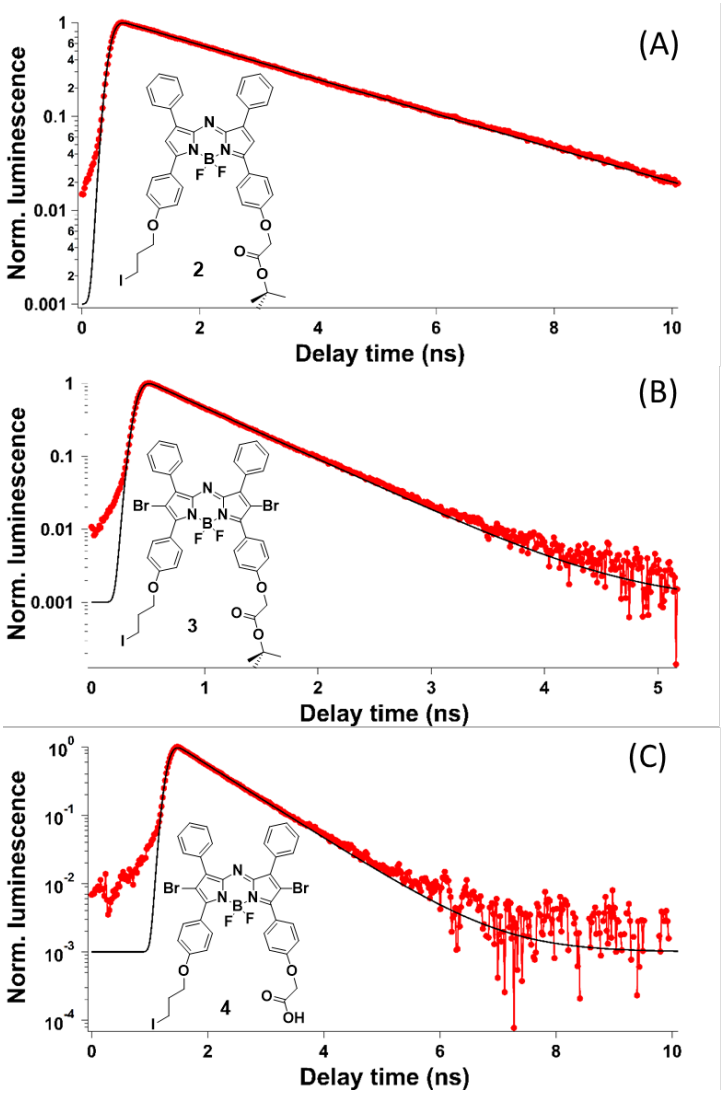

Figure S24. Time-resolved emission decay of PS (A) **2** (C) **3** and (C) **4** in THF (λ_{exc} = 630 nm, λ_{ob} = 700 nm).

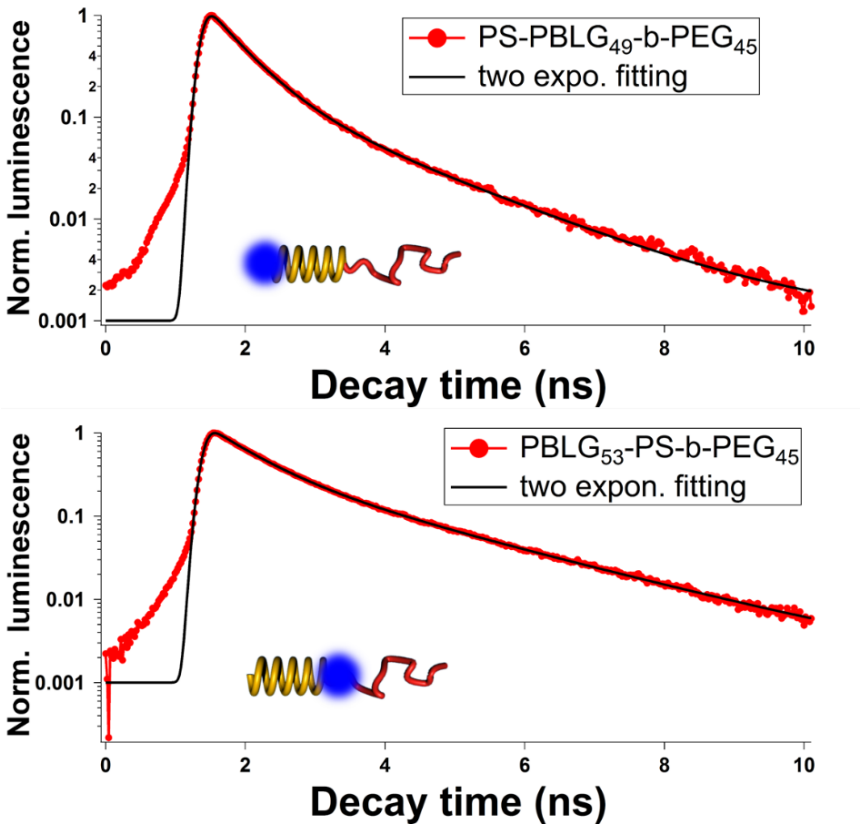

Figure S25. Time-resolved emission decays of PS-PBLG-*b*-PEG and PBLG-PS-*b*-PEG type block copolymers in THF (λ_{exc}=630 nm, λ_{ob}=700 nm), with biexponential fit.

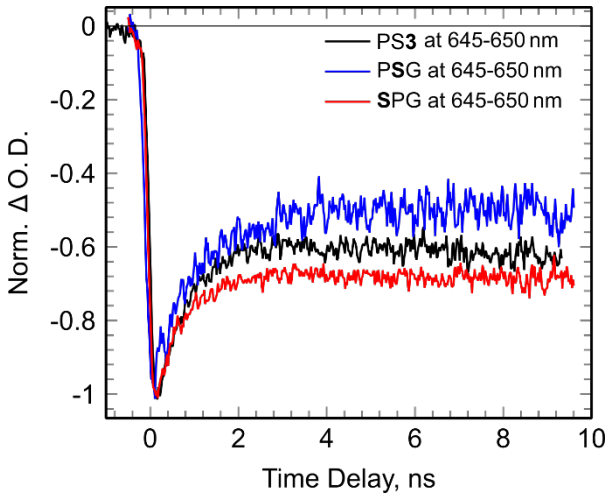

Figure S26. Evolution of transient signals of excited PS **3**, P**S**G, **S**PG at 645-650 nm in THF (λ_{exc}=630 nm).

Figure S26 shows ground state bleaching recovery of excited PS **3**, P**S**G, **S**PG samples in THF, which allows calculation of the yield of formation of triplet state due to intersystem crossing in the polymer-grafted PS. Incomplete relaxation of the signals gives evidence of formation of a long-lived metastable state, which in conjunction with fluorescence quenching kinetics of the Aza-BODIPY chromophore confirm rapid and efficient population of the active triplet state in the studied samples.

2.6.3 Singlet oxygen generation measurement in DCM

The singlet oxygen luminescence spectra were recorded in air saturated DCM solutions with 630 nm excitation wavelength with an Innolas MOPA-1 variable repetition rate (1–5000 Hz) Nd:YAG laser. The measurements were performed on a Horiba Jobin-Yvon Fluorolog-3 equipped with a Hamamatsu H10330–45 NIR detector configured with a Fastcom P7889 100 ps multistop TDC acquisition card operating at 10 GHz. As a reference, an optically matched solution of methylene blue (MB) was used (Φ_{Δ}=0.57 in DCM). [8,9a,b] The optical density of the reference MB and the samples at excitation wavelength were adjusted to 0.1 in DCM and

excited with 630 nm light. The relative singlet oxygen generation quantum yields were calculated from equation 4. by using optically matched photosensitizer.

$$\Phi_{\Delta}^{x} = \Phi_{\Delta}^{R} \frac{I_x}{I_R} \frac{A_R}{A_x} \frac{\tau_R}{\tau_x} \quad (4)$$

Where I is the emission intensity of $^1O_2$ (at 1270 nm), A is the absorption of the solution, τ is the lifetime of the $^1O_2$ phosphorescence in the selected solvent, X and R indices refer to the sample and reference compound, respectively. [10]

Measurements were performed in air-equilibrated solutions.

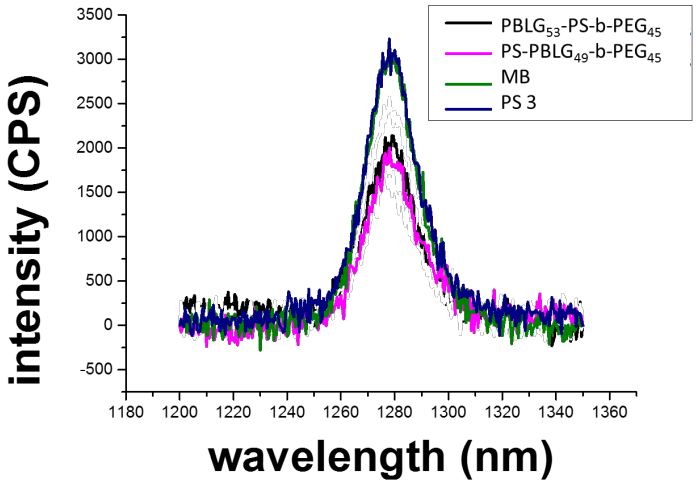

Figure S27. Luminescence of the $^1O_2$ generated by PS functionalized block copolymers, PS 3 and Methylene blue (MB) in DCM (dilute solutions, OD 0.1, λ_{ex}=630 nm).

2.6.4 The singlet oxygen generation measurement of nanoparticles in water

The quantum yields of singlet oxygen production (Φ_{Δ}) of PS bearing self-assemblies in water were calculated according to the literature.[9] An optically matched photosensitizer, methylene blue was selected as a reference sensitizer with known Φ_{Δ} (0.52) in water.[9] The absorption of PTS in the nanoparticles was adjusted to 0.1 (2 x 10^{-5} M) and the absorption of trapping molecule, AVS was adjusted to 1.2 (6.5 x 10^{-5} M) in the nanoparticles solution in 1 cm quartz cuvette. The absorption spectra were taken in dark over 10 min and after each 5 min excitation time with 660 nm LED over a time period of 1 h. Photodegradation rate of the AVS at 395 nm was subtracted from the spectrum and Φ_{Δ} were calculated from equation 5, respectively.

$$\Phi_{\Delta}^{x} = \Phi_{\Delta}^{R} \left(\frac{m_x}{m_R} \frac{F_R}{F_x}\right) \quad (5)$$

Where *m* is the photobleaching rate of the trap molecule and *F* is the optical density of PTS at irradiation wavelength, X and R indices refer to the sample and reference compound, respectively.

All measurements were performed in air-equilibrated solutions.

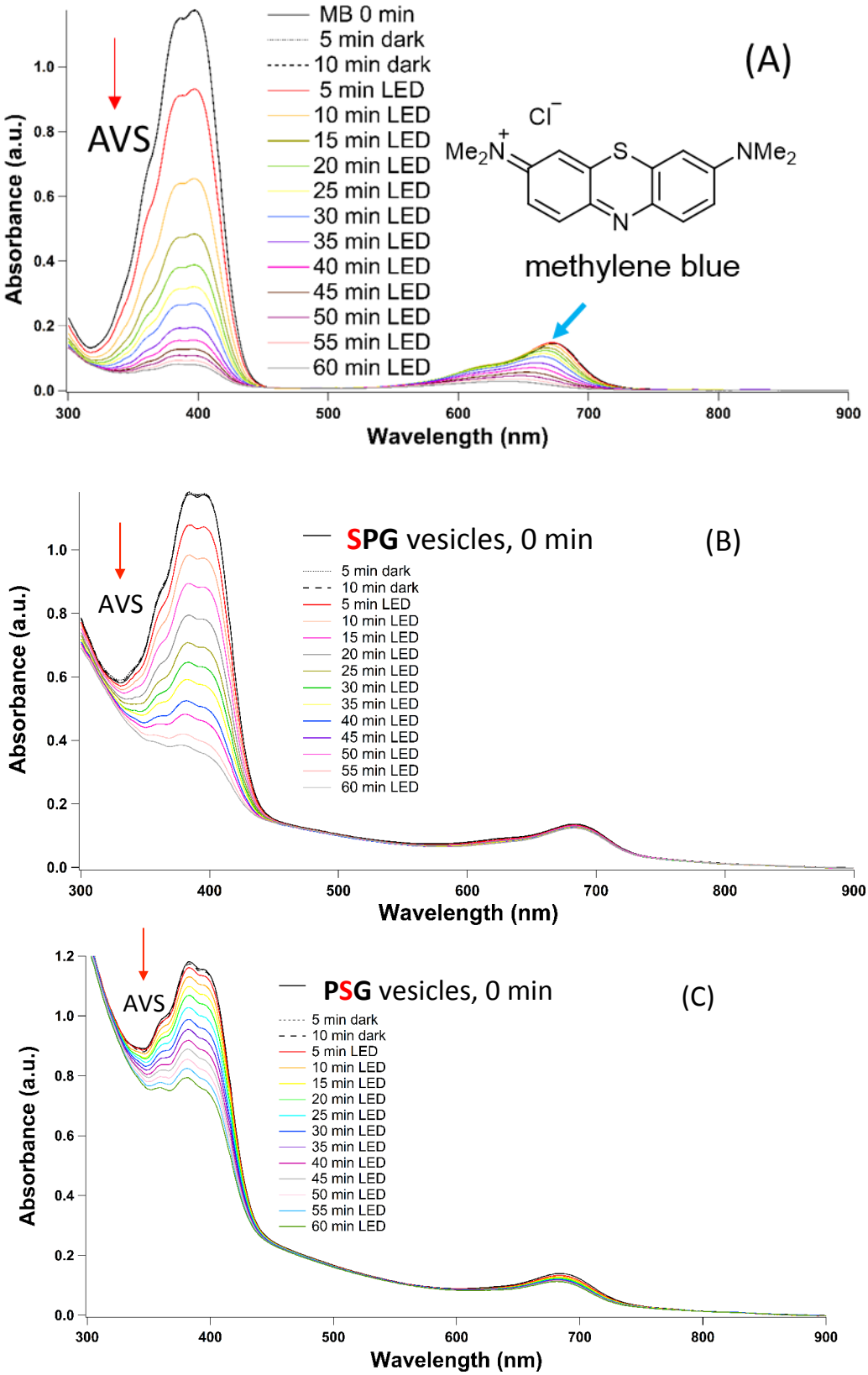

Figure S28. Overlay of UV-Visible spectra of an irradiated solution of AVS in the presence of (A) Methylene Blue; (B) PS-PBLG$_{49}$-*b*-PEG$_{45}$ vesicles and (C) PBLG$_{53}$-PS-*b*-PEG$_{45}$ vesicles.

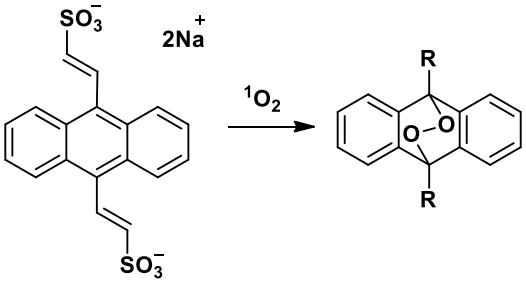

Scheme S3: [4+2] cycloaddition reaction of 9,10-bis-(vinylsulfonate)anthracene (AVS) with $^1O_2$

2.7 In vitro studies

2.7.1 Cell Culture

For in vitro tests two human cell lines: cervix cancer cells HeLa and skin cancer cell line B16F1 were used. HeLa cells were cultured at 37 °C for 24 hours in Minimum Essential Medium (MEM) supplemented with 10% heat-inactivated FBS and 100U/mL penicillin–streptomycin, in 5% CO_2-humidified atmosphere. B16F1 cells were cultured at 37 °C for 24 hours in minimum essential medium (MEM Alpha Medium (1X)+ GlutaMax) supplemented with 10% heat-inactivated FBS and 100U/mL penicillin–streptomycin, in 5% CO_2-humidified atmosphere.

2.7.2 Cellular uptake

Cellular uptake of nanocarriers was quantified by flow cytometry. HeLa and B16F1 cells were seeded in two different 24-well plates (5×10^4 cells/ well) 24 h before the experiment. Cells were incubated with nanocarriers for 4 and 24 h at concentrations of 1, 0.5, 0.25, 0.125, 0.062 mg/mL. Then, cells were rinsed with phosphate-buffered saline (PBS) solution, trypsinized and diluted with cell medium. After centrifugation (250 RPM, 5 min, 4 °C), the cell pellet was resuspended in 200 µL PBS. The measurements were done on a FACSCalibur cytometer (BD Biosciences, Erembodegem, Ex: 640 nm Em: 660 nm). After obtaining the best internalization at 24 h the experiment was repeated two more times for 24 h incubation time at concentrations of 1, 0.5, 0.25, 0.125, 0.062 mg/mL. Finally, the data were analyzed using Flow Jo software. 5×10^3 cells were analyzed in each measurement.

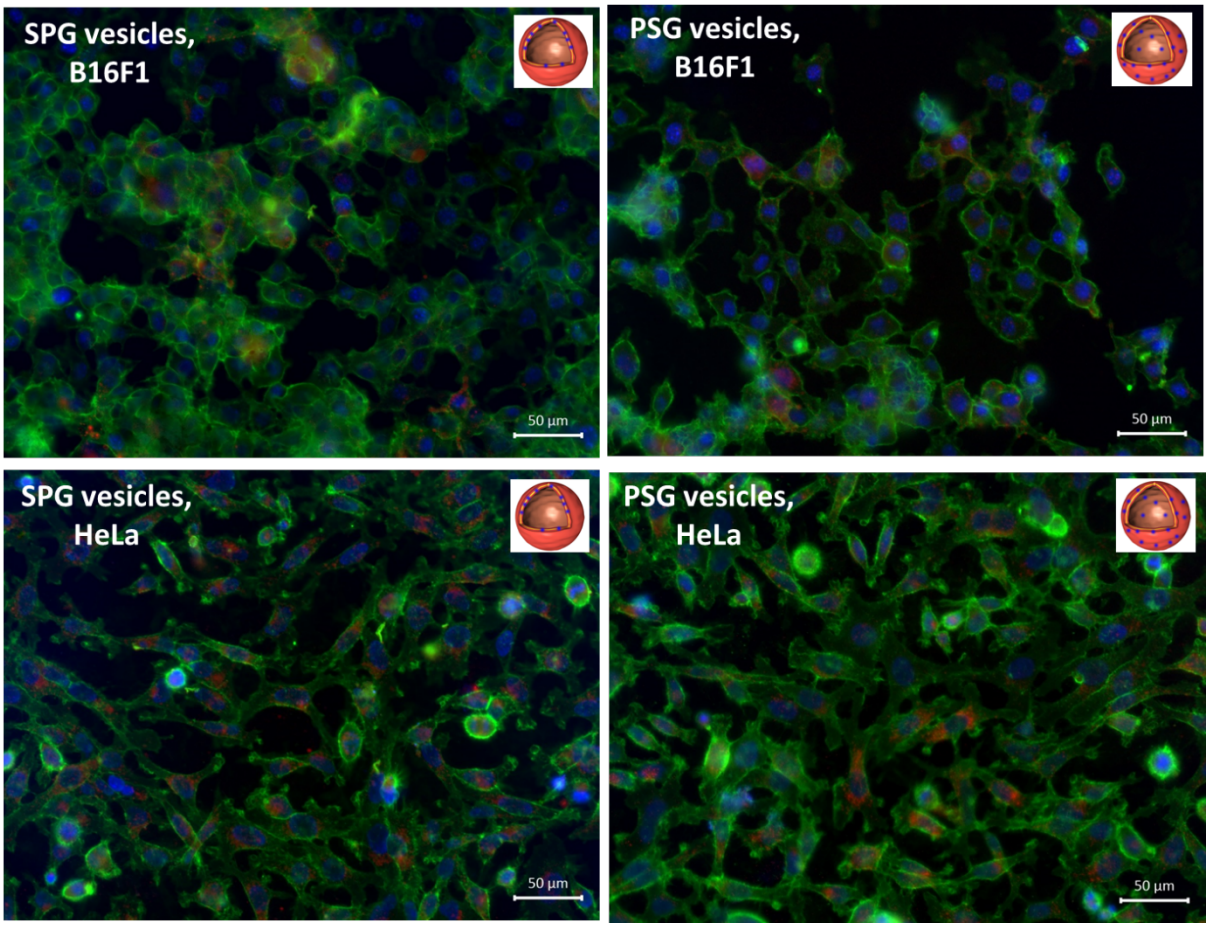

Figure S29. Confocal laser scanning microscopy (CLSM) images of B16F1 and HeLa cells incubated with vesicles over 24 h. Blue fluorescence is due to the nuclei staining with 4,6-diamidino-2-phenylindole (DAPI), green fluorescence is due to the membrane staining with AlexaFluor488-conjugated concanavalin A and red fluorescence is due to the PS fluorescence in the vesicles. The level of fluorescence in the images has not been normalized,

2.7.3 Cell viability in dark

The HeLa and B16F1 cells were seeded on two different 96-well plate and incubated for 24 h at 37°C. Then the cells were incubated with 1 mg/mL and 0.5 mg/mL nanocarrier solutions for 24 h. After the cells were washed with cell medium and 0.5 mg/mL of MTT solution was added and the cells were incubated for 3 h. The formazan that is produced in the cells was dissolved in 100 µL dimethylsulfoxide (DMSO) and read at 560 nm wavelength via Multiskan Ex plate reader (Thermo Fisher Scientific).

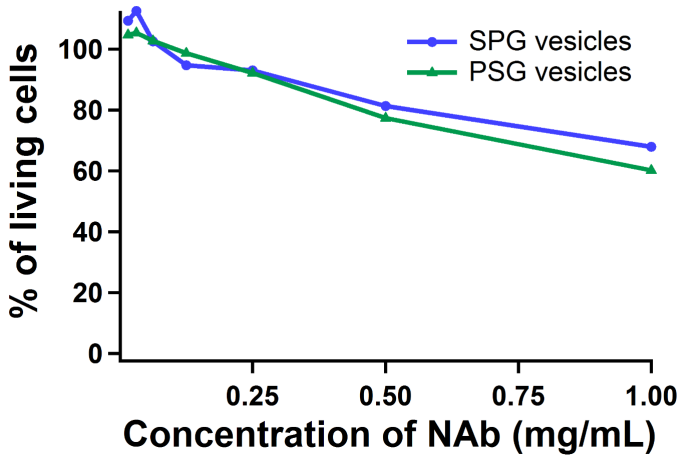

Figure S30. Cytotoxicity tests of the nanocarriers (NAb) as a function of concentration on HeLa cells (in dark, n=1).

2.7.4 Cell viability after LED irradiation (in vitro PDT)

The HeLa and B16F1 cells were seeded on two different 96-well plates and incubated for 24 h at 37°C. Then the cells were incubated with 1 mg/mL and 0.5 mg/mL nanocarrier solutions for 24 h. To activate the photosensitizers in the nanocarriers the plates were irradiated with LED light (660 nm, power density 1.33 mW/cm^2) for 15, 30 and 60 min. The cells were incubated 24 more hours and to identify the cell viability 0.5 mg/mL of MTT solution was added and the cells were incubated for 3 h. The formazan that is produced in the cells were dissolved in 100 µL dimethylsulfoxide (DMSO) and read at 560 nm wavelength via Multiskan Ex plate reader.

We observed the similar behavior in both cell line. In two cases, P*S*G vesicles exhibited higher toxicity compare to *S*PG vesicles at low concentration.

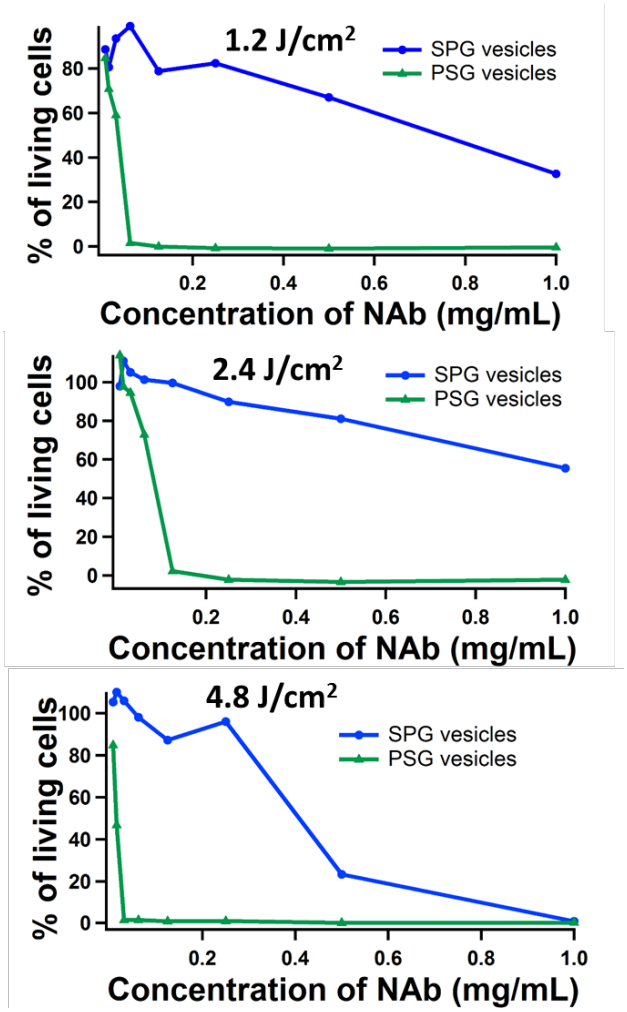

Figure S31. Cytotoxicity tests of the nanocarriers (Nab) under 660 nm LED irradiation as a function of light dose and nanocarrier concentration (HeLa cells, n=1).

References

[1] a) G. De Bo, J. De Winter, P. Gerbaux, C.A. Fustin, *Angew. Chem. Int. Ed.* **2011**, *50*, 9093; b) A. Van Quaethem, P. Lussis, D.A. Leigh, A.S. Duwez, C.A. Fustin, *Chem. Sci.* **2014**, *5*, 1449.

[2] a) P.Batat, M. Cantuel, G. Jonusauskas, L. Scarpantonio, A. Palma, D. F. O'Shea, N. D. McClenaghan, *J. Phys. Chem. A* **2011**, *115*, 14034.; b) V. Lebrun, A. Tron, L. Scarpantonio, C. Lebrun, J.-L. Ravanat, J.-M. Latour, N. D. McClenaghan, O. Sénèque, *Angew. Chem. Int. Ed.* **2014**, 53, 9365.

[3] S. Denisov, Ph. D. thesis, Université de Bordeaux, 2014.

[4] a) A. Gorman, J. Killoran, C. O'Shea, T. Kenna, W. M. Gallagher, D. F. O'Shea, *J. Am. Chem. Soc.* **2004**, *126*, 10619.; b) D. Wu, S. Cheung, R. Daly, H. Burke, E. M. Scanlan, D. F. O'Shea, *European Journal of Organic Chemistry* **2014**, *2014*, 6841.

[5] K. Greish, In *Cancer Nanotechnology: Methods and Protocols*, (Eds.: R. S. Grobmyer, M. B. Moudgil), Humana Press, Totowa, NJ, 2010, pp. 25.

[6] S. Schöttler, G. Becker, S. Winzen, T. Steinbach, K. Mohr, K. Landfester, V. Mailänder, F. R. Wurm, *Nat. Nano.* **2016**, *11*, 372.

[7] J. C. de Mello, H. F. Wittmann, R. H. Friend, *Adv. Mater.* **1997**, *9*, 230.

[8] T. Yogo, Y. Urano, Y. Ishitsuka, F. Maniwa, T. Nagano, *J. Am. Chem. Soc.* **2005**, *127*, 12162.

[9] a) Y. Cakmak, S. Kolemen, S. Duman, Y. Dede, Y. Dolen, B. Kilic, Z. Kostereli, L. T. Yildirim, A. L. Dogan, D. Guc, E. U. Akkaya, *Angew. Chem., Int. Ed.* **2011**, *50*, 11937; b) B. Kilic, N. Yesilgul, V. Polat, Z. Gercek, E. U. Akkaya, *Tetrahedron Letters* **2016**, *57*, 1317.

[10] F. Wilkinson, W. P. Helman, A. B. Ross, *J. Phys. Chem. Ref. Data* **1993**, *22*, 113..